
ITERATIVE GRAPH NEURAL NETWORK ENHANCEMENT VIA FREQUENT SUBGRAPH MINING OF EXPLANATIONS

A PREPRINT

✉ **Harish G. Naik**

Department of Computer Science
University of Illinois at Chicago
hnaik2@uic.edu *

Jan Polster

Department of Computer Science
University of Bonn
s6japols@uni-bonn.de

Raj Shekhar

Department of Computer Science
University of Illinois at Chicago
rshekh3@uic.edu †

Tamás Horváth

Dept. of Computer Science, University of Bonn
Fraunhofer IAIS, Sankt Augustin
Lamarr Institute for
Machine Learning and Artificial Intelligence
horvath@cs.uni-bonn.de ‡

György Turán

University of Illinois at Chicago
HUN-REN-SZTE Research Group on AI, Szeged
gyt@uic.edu §

March 13, 2024

ABSTRACT

We formulate an XAI-based model improvement approach for Graph Neural Networks (GNNs) for node classification, called Explanation Enhanced Graph Learning (EEGL). The goal is to improve predictive performance of GNN using explanations. EEGL is an iterative self-improving algorithm, which starts with a learned “vanilla” GNN, and repeatedly uses frequent subgraph mining to find relevant patterns in explanation subgraphs. These patterns are then filtered further to obtain application-dependent features corresponding to the presence of certain subgraphs in the node neighborhoods. Giving an application-dependent algorithm for such a subgraph-based extension of the Weisfeiler-Leman (1-WL) algorithm has previously been posed as an open problem. We present experimental evidence, with synthetic and real-world data, which show that EEGL outperforms related approaches in predictive performance and that it has a node-distinguishing power beyond that of vanilla GNNs. We also analyze EEGL’s training dynamics.

1 Introduction

XAI-based model improvement is a relatively recent research direction in XAI. The underlying observation is that explanations, besides providing information to the user about the model’s decision, can also be used to improve the model. A recent survey is given in [28].

In this paper we consider Graph Neural Networks (GNNs) for node classification within the XAI-based model improvement paradigm. Message-passing GNNs (MPNNs)⁵ have limited representational power due to the limitations

*This publication is based on work supported in part by the University of Illinois at Chicago and the National Science Foundation (NSF) award #CNS-1828265 for MRI: Acquisition of a Composable Platform as a Service Instrument for Deep Learning & Visualization (COMPaaS DLV).

†Supported by NSF grants 1828265 and 2217023

‡This research has been funded by the Federal Ministry of Education and Research of Germany and the state of North Rhine-Westphalia as part of the Lamarr Institute for Machine Learning and Artificial Intelligence.

§Partially supported by NSF grants 2217023, 2240532 and by the AI National Laboratory Program (RRF-2.3.1-21-2022-00004).

⁵A note on graph neural network terminology: GNN is the general term, [8] uses MPNN and [18] uses GCN. We use these terms depending on context.

of the related Weisfeiler-Leman (1-WL) algorithm [23, 29]. Two nodes which are indistinguishable by 1-WL are indistinguishable by any MPNN.

Extending the power of MPNN to overcome these limitations is a fundamental challenge. One approach is higher-order variants of WL, which are more expressive, but computationally less tractable [11]. Another approach is to add structural information as node features. For vanilla MPNN node feature vectors are constant. The number of triangles in the 1-hop neighborhood of a node, which cannot be detected by 1-WL, can be such an added feature. In [9], the authors propose adding node features by counting the number of rooted subgraphs that are isomorphic to a given rooted pattern graph. They suggest domain-specific patterns, e.g., cliques for social networks and cycles for molecules. Adding new features by counting the number of rooted homomorphisms is proposed in [8]. Building on these proposals, a general question, formulated in [8], is how to select useful patterns? We refer to this problem as the GNN pattern selection problem. It is noted in [8] that “one important remark is that selecting the best set of features is still a challenging endeavor”. They also point out that the application-dependence of the best set of features adds to the difficulty of the problem.

In this paper we propose an approach to the GNN pattern selection problem for *application-dependent* features, i.e., the features are extracted from the data in an automatic way, and *not* by using some domain-specific pattern set. XAI-based model improvement suggests to use explanations for solving the GNN pattern selection problem. Utilizing that explanations for GNNs are often rooted subgraphs, we propose the EXPLANATION ENHANCED GRAPH LEARNING (EEGL) approach for iterative enhancement of the predictive performance of GNNs for node classification. EEGL uses frequent connected subgraph mining to identify patterns occurring in many explanation subgraphs for nodes of a given class. These are analyzed further to select the best patterns. Nodes are then annotated with features based on the presence or absence of these patterns in the neighborhood. Starting with vanilla GNN, the process can be iterated.

A few remarks are in order about assumptions underlying the approach and its intended scope of applications. It is assumed that the learning problem is such that 1. there exist explanation subgraphs of reasonable quality and 2. the GNN learning and explanation algorithm to be improved is of reasonable quality. The *hypothesis* underlying our work, then, is that if assumptions 1. and 2. hold then explanations can be used to construct useful features, and those can be used to improve performance. Assumptions 1. and 2. are not expected to hold in general. On the other hand, assumption 2. is not too restrictive as the goal is *to improve a weak learner using weak explanations*, a setup which may be of interest in itself. Applications where the assumptions may hold could be in scientific discovery. A scientist could suggest a kind of explanation to the data scientist, who could use EEGL to evaluate, use or correct this suggestion [24].

For the experimental evaluation of the EEGL approach, one can consider the following questions:

- Q1: Can the node-distinguishing power and hence, the predictive performance of GNNs be improved by using frequent subgraph mining of explanations? Do iterations help?
- Q2: How does the performance of EEGL-trained GNNs compare to other feature initializations and subgraph-based GNNs?
- Q3: What is the effect of the relationship between 1-WL symmetries and label partitions?

Summary of the Experimental Results The objective of the paper is to provide first steps towards answering these questions, focusing on the effect of *structural complexity*. One should note that our approach is not expected to be applicable in cases when the information provided by the graph is more of a statistical nature, as in social networks. In contrast, motivated by the connections to 1-WL, we consider synthetic and real-world datasets with different relationships between the node classes having the same 1-WL labels and those having the same class labels. From this point of view, datasets studied belong to three categories: (i) The graph has a large number of 1-WL classes, compared to its size (*low* 1-WL symmetry) and target classes are formed by the union of a family of 1-WL classes, (ii) the graph has a small number of 1-WL classes, compared to its size (*high* 1-WL symmetry) and all 1-WL classes are formed by the union of a family of target classes, and its special case that (iii) the graph is regular (each node has the same degree) and has therefore only one 1-WL class. We used synthetic datasets for (i) and (ii), and *fullerenes* for (iii). The following are some of the main conclusions of our experiments.

Answer to Q1: EEGL was capable of iterative self-improvement from explanations in at most 3 iterations on *all* learning tasks considered, including those that require a node-distinguishing power beyond that of vanilla GNNs.

Answer to Q2: We considered three other feature initializations: (1) one-hot encoding of true class labels (regarded as an upper bound on the performance of GNN on the learning task), (2) randomly assigned numerical features [1, 10], and (3) “maliciously” selected subgraph features (motivated by the comment of [8] that performance

“almost always benefits from any set of additional features”). We also compared EEGL’s predictive performance to that of SHADOW-GNN [31], a subgraph-based approach which also generates node representations *dynamically*. EEGL *outperforms* (2) and (3) and SHADOW-GNN on all datasets, except for one, where SHADOW-GNN achieved approximately the same F1-score.

Answer to Q3: EEGL performed well on datasets of all three types. Its predictive performance was close to 100% on all problems in (i) and (ii). Regarding (iii), EEGL achieved 100% on most and between 86 and 97% on 3 fullerenes, most in the first iteration. It was, however, unable to improve the results on the 3 fullerenes in the subsequent rounds. EEGL achieved already more than 99% in average in one iteration on all problems in category (i) and 97% in category (iii). For the dataset in category (ii), it needed three iterations to achieve 100%.

Contributions In summary, the main contribution of this work is a general *self-improving* framework to overcome the inherent limited representational power of vanilla GNNs. In particular, it (i) applies an XAI-based iterative model improvement method to GNN, (ii) provides an automated, application-dependent solution to the GNN pattern selection problem, (iii) applies frequent connected subgraph mining to XAI, and (iv) gives a detailed study of node classification problems where graph-theoretic structural complexity is relevant.

Outline The rest of the paper is organized as follows. In Sections 2 we overview related work. The EEGL system is presented in Section 3. We report and discuss the experimental results obtained in Section 4. Finally, in Section 5 we conclude and formulate some problems for further research.

2 Related Work

Besides the most closely related works, already cited in Section 1, we briefly mention some further references, using survey papers covering related work when possible. A recent general survey of XAI, including some discussion of the role of XAI-based model improvement, is [6]. In the survey of [22] of the different variations of the Weisfeiler-Leman algorithm, Section 5.2 is about neural architectures extending 1-WL, including [8, 9]. A subsection discusses other subgraph-enhanced approaches, including SHADOW-GNN [31] on node classification, which implement symmetry-breaking to address the limitations of 1-WL (see Appendix B). Thus these approaches exploit properties of the network, but do *not* take the learning problem into consideration (with the exception of [31]). A detailed computational study is given in [11], including results on k -WL. The need for synthetic examples is discussed in [20].

Explanatory interactive machine learning [14, 15] considers explanations returned by the learner and corrected by the user as part of the human-in-the-loop learning process. Faithfulness, a basic metric for evaluating explanations, measures the predictive power of explanation subgraphs [4]⁶. Other works, closer to the present paper, use explanations in an automated manner as a tool for improving prediction. In [5] the effect of incorporating linear approximations into the learning process is considered. Similarly, [3] uses explainability information to guide message passing in GNN. The SUGAR system [27] uses a reinforcement pooling mechanism to incorporate significant subgraphs into graph classification.

3 The EEGL System

Before presenting the main components of the EXPLANATION ENHANCED GRAPH LEARNING (EEGL) system, we first recall some necessary notions. Background on GNN, GNNEXPLAINER, Weisfeiler-Leman algorithm, and frequent subgraph mining is given in [16, 26, 30] and Appendix A.

Notions and Notation For a graph G , $V(G)$ and $E(G)$ denote the sets of nodes and edges. Graphs are always undirected. A rooted graph is a pair (G, v) , where $v \in V(G)$. Graph G_1 is *isomorphic* to graph G_2 if there is a *bijection* $\psi : V(G_1) \rightarrow V(G_2)$ such that $\{u, v\} \in E(G_1)$ iff $\{\psi(u), \psi(v)\} \in E(G_2)$ for all $u, v \in V(G_1)$. Furthermore, G_1 is *subgraph isomorphic* to G_2 if G_2 has a subgraph that is isomorphic to G_1 , or equivalently, if there exists an *injective* function $\varphi : V(G_1) \rightarrow V(G_2)$ such that $\{\varphi(u), \varphi(v)\} \in E(G_2)$ if $\{u, v\} \in E(G_1)$, for all $u, v \in V(G_1)$. A rooted graph (G_1, r) has a *rooted subgraph isomorphism* into a rooted graph (G_2, v) if there is a subgraph isomorphism φ from G_1 into G_2 such that $\varphi(r) = v$. A *rooted pattern* is a pair (P, v) such that P is a connected graph and $v \in V(P)$. The 1-WL algorithm [16] defines a partition of $E(G)$ of a graph G . The blocks of this partition will be referred to as the *1-WL classes* of G . Nodes u, v of G belong to the same *orbit* of G iff there is an automorphism (i.e., isomorphism from G to G) mapping u to v . The orbits define an equivalence relation over $E(G)$, which is a refinement of the equivalence relation defined by the 1-WL classes.

⁶Another comment on terminology: in this paper we do not discuss the evaluation of explanations. Thus we mean accuracy in the standard ML, and not in the XAI sense, as used in [4] and somewhat differently in [30].

Algorithm 1 EXPLANATION ENHANCED GRAPH LEARNING

Parameters: feature vector dimension d , iteration number K , set C of class labels

Input: graph G with n vertices, set $T \subseteq V(G) \times C$ of training examples, relative frequency threshold $\tau \in (0, 1]$
Output: GNN model $\Phi : V(G) \rightarrow C$

```

1:  $X \leftarrow \text{INIT\_FEATURE\_MATRIX}(G, d)$ 
2: for  $k = 1, \dots, K$  do
3:    $\Phi \leftarrow \text{GNN\_LEARNING}(G, X, T)$ 
4:   for all  $c \in C$  do  $\mathcal{E}_c \leftarrow \emptyset$ 
5:   for all  $v \in V(G)$ 
6:      $E_v \leftarrow \text{GNN\_NODE\_EXPLAINER}(G, X, \Phi, v)$ 
7:     add  $E_v$  to  $\mathcal{E}_c$ , where  $c = \Phi(v)$ 
8:   for all  $c \in C$  do
9:      $\mathcal{P}_c \leftarrow \text{MAXIMAL\_FREQUENT\_PATTERNS}(\mathcal{E}_c, \tau)$ 
10:   $\mathcal{P}^\top \leftarrow \text{TOP\_PATTERNS}(\mathcal{P}, \min\{d, |\mathcal{P}|\}, T)$ , where
       $\mathcal{P} = \bigcup_{c \in C} \mathcal{P}_c$ 
11:   $X \leftarrow \text{UPDATE\_FEATURE\_MATRIX}(G, \Phi, \mathcal{P}^\top, d)$ 
12: return  $\Phi$ 
    
```

The EEGL System The pseudocode of EEGL is given in Alg. 1 (see, also, Fig. 6 in Appendix C for a high-level depiction) It consists of the (i) GNN learning, (ii) node explainer, (iii) pattern extraction, and (iv) feature annotation modules. The four modules are used to learn an unknown target function $f : V(G) \rightarrow C$, where G is the input graph and C is a finite set of class labels. In addition to G , the input to EEGL also contains a set $T = \{(v, f(v)) : v \in V'\}$ of training examples for some $V' \subseteq V(G)$, the dimension d of the node feature vectors, a relative frequency threshold $\tau \in (0, 1]$, and a positive integer K specifying the number of iterations (cf. Alg. 1). In each iteration of the outer loop in Alg. 1 (lines 2–11), all nodes of G are associated with a d -dimensional *feature vector*. The feature vectors of the nodes are represented by an $n \times d$ *feature matrix* X , where $n = |V(G)|$. We now describe the above four modules.

GNN Learning Module (line 3 of Alg. 1) In each iteration, EEGL first learns a new GNN Φ for G using G , X , and T as input. While G and T are unchanged, X is recalculated in each iteration. It is initialized in line 1 and updated in line 11. In case of the “vanilla” initialization, X is set to the $n \times d$ matrix of ones. The function GNN.LEARNING (line 3) is realized with GCN [18].

Node Explainer Module (lines 4–7 of Alg. 1) The GNN model Φ is used as input to the *node explainer* module, together with G and X . It is called for each $v \in V(G)$ separately (lines 5–6) and returns an *individual* subgraph E_v of G as the explanation for the model’s prediction of the class of v by $\Phi(v)$. In our experiments, the node explainer function GNN.NODE.EXPLAINER (line 6) is realized with the GNNEXPLAINER system [30]. The explanation graphs returned by GNNEXPLAINER contained the nodes themselves.⁷ Node v is marked as the *root* of E_v . We note that GNNEXPLAINER also calculates a feature mask for each explanation pattern. These are disregarded in EEGL but could play a role in future work. The explanation graphs are partitioned according to the class labels *predicted* by Φ (lines 4 and 7); the block containing the explanation graphs for a class $c \in C$ is denoted by \mathcal{E}_c (cf. line 7).

Pattern Extraction Module (lines 8–10) This module generates a set of *maximal frequent rooted* patterns from the explanation graphs computed by the previous module. This will then be used by the next module. The underlying assumption behind the synthetic and real-world examples is that there is a set of *class patterns* for each class label. More precisely, for input graph G , target function f , and class label $c \in C$ there is a set S_c of (almost) *contrastive* rooted patterns such that (i) for most⁸ $v \in V(G)$ with $f(v) = c$, there is a rooted pattern $(P_c, r_c) \in S_c$ and a rooted subgraph isomorphism from (P_c, r_c) to (G, v) and (ii) there is *no* such rooted pattern in S_c and rooted subgraph isomorphism for *most* $v' \in V(G)$ with $f(v') \neq c$. The set S_c is the underlying *ground truth*.

Let $v \in V(G)$ be a node selected uniformly at random such that $\Phi(v) = c$ for some $c \in C$ and let (P_c, r_c) be a rooted pattern from S_c . It follows from the assumptions that with a certain probability, a rooted explanation graph $(P_v, v) \in \mathcal{E}_c$ computed for v contains a subgraph P'_v such that $v \in V(P'_v)$ and (P'_v, v) is a rooted subgraph of (P_c, r_c) (i.e., there is a rooted subgraph isomorphism from (P'_v, v) to (P_c, r_c)). Since P'_v is a subgraph of P_v and rooted subgraph isomorphism is used for pattern matching, (P'_v, v) contains *less* structural constraints. Hence, it can

⁷Parameters can be chosen so that GNNEXPLAINER [30] is forced to include v in E_v for *all* $v \in V(G)$.

⁸The qualifications almost, most refer to both noise in the data and errors in prediction and explanation.

be regarded as a *generalization* of (P_v, v) .⁹ Thus we need to calculate a set of rooted patterns that generalize a large fraction of the rooted explanation graphs in \mathcal{E}_c and, in order to avoid redundancy, are *most specific* with respect to this property. As mentioned above, there are two sources of errors for the explanation patterns computed by the previous module. First, with a certain probability, the true class label $f(v)$ is predicted *incorrectly* by Φ (i.e., $f(v) \neq c = \Phi(v)$). Second, there is *no* guarantee that the explanation graph (P_v, v) provides a *genuine* explanation for predicting the class label of v by $\Phi(v) = c$, independently whether or not $\Phi(v) = f(v)$. Still, it is reasonable to assume that many of the *individual* explanation patterns computed for c have a relatively large overlap with some unknown class patterns in S_c . Accordingly, we expect that *most frequent* rooted subgraphs of \mathcal{E}_c computed in the node explanation module are rooted *subgraphs* of some patterns in S_c .

The above arguments motivate considering the *maximal frequent* rooted subgraphs of \mathcal{E}_c (i.e., which are frequent and all their proper connected supergraphs are infrequent in \mathcal{E}_c w.r.t. τ) (line 9). The assumptions imply that they contain at least a part of the structural information assigning a node to class c . These patterns can be regarded as the *most specific generalizations* of most of the individual explanations in \mathcal{E}_c . (For more details please see Appendix D.)

After the computation of the maximal frequent rooted subgraphs for all $c \in C$ (lines 8–9), a small subset \mathcal{P}^\top of *top* rooted patterns is selected from $\mathcal{P} = \bigcup_{c \in C} \mathcal{P}_c$ (line 10). More precisely, for each $(P, r) \in \mathcal{P}_c$, EEGl evaluates how well (P, r) performs as a classifier for class c by computing its F1-score on the training set T . The module then returns the top d' patterns with the highest F1-scores in a round-robin fashion from \mathcal{P} , where $d' = \min\{d, |\mathcal{P}|\}$.

Feature Annotation Module (line 11) Using the rooted patterns $(P_1, r_1), \dots, (P_{d'}, r_{d'})$ returned by the pattern extraction module, in this module we update X for the next iteration of the main loop by setting $\vec{x}_v[j]$ to 1 if there is a rooted subgraph isomorphism from (P_j, r_j) to (G, v) ; otherwise to 0, for all $v \in V(G)$ and $j \in [d']$. If $d' < d$, the last $d - d'$ entries in \vec{x}_i are set to some constant.

4 Experimental Evaluation

In this section we present our experimental results evaluating the predictive performance of EEGl on synthetic and real-world graphs and address the questions formulated in Sect. 1. All learning tasks are themselves or are reduced to node classification tasks. The use of synthetic data is also justified by [20], discussing the state of the art on node classification benchmarks. The focus of [20] is on parameters such as class size distributions, and edge densities between classes (corresponding to heterophily versus homophily). In contrast, we are interested in the effect of structural complexity. The experiments are grouped into three blocks, depending on the relationships between the graphs' 1-WL and target classes, determined by the graph structures and the class labels, respectively.

4.1 Experimental Setup and Runtimes

Recall from Section 3 that the input graph G with n nodes is associated with a feature matrix of size $n \times d$. For each graph G used in the experimental evaluation, we carried out different experiments with GCN [18], SHADOW-GNN [31], and our EEGl system. The GCN experiments use precomputed feature vectors. In particular, in the *label encoding* setting, feature vectors are essentially one-hot encodings of the node labels. In the *adversarial* setting, feature annotation is done with a precomputed set of adversarial rooted patterns constructed for the ground truth patterns. In the *randomized* setting, feature annotation is done using precomputed random numbers from $[0, 1]$. Motivation for choosing these settings and discussion of the experiments are given in Sections 4.2–4.4.

Parameters Regarding the parameters, we used different values for d , depending on the number of target classes. Our realization of EEGl uses GASTON [25] to generate the candidate frequent patterns. This subroutine has a frequency threshold parameter τ . We used $\tau = 0.7$ for the datasets in Sections 4.2, 4.3 and $\tau = 0.1$ for the fullerenes in Sect. 4.4. The GCN model and training parameters (size of hidden layers, dropout rate, number of epochs, learning rate, and weight decay) were chosen by hyperparameter grid search. Recall from Sect. 3 that in case of vanilla initialization, X is set initially to the matrix of ones. The learning step in the initial round can therefore be regarded as learning a vanilla GNN because the feature matrix provides *no* information. It is therefore not counted as an EEGl round and will be referred to as round 0 or R0. Using this terminology, we carried out at least one iteration with EEGl in all experiments. The same applies to EEGl with random initialization. Finally, for all experiments with GCN, SHADOW-GNN, and EEGl, we used k -fold cross validation (CV) for $k = 5$ or 10, depending on graph size.

Implementation Details Experiments showed that the performance of EEGl framework is highly influenced by the choice of the classifier and the explainer implementations. We noticed that for the synthetic dataset derived by addition

⁹By generalization we mean the relationship between two rooted patterns in the poset of all rooted patterns defined by rooted subgraph isomorphism, and *not* “generalization” from data as used in machine learning.

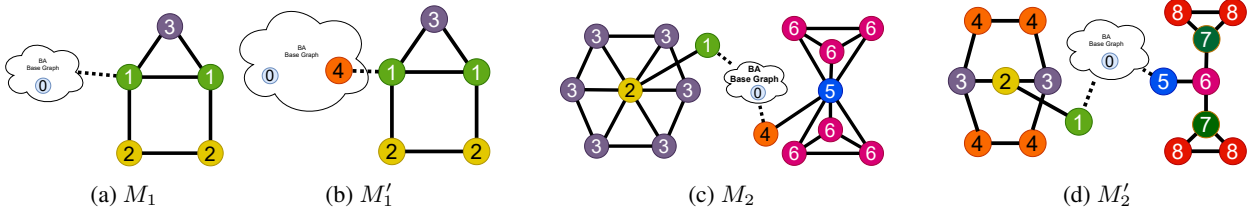


Figure 1: The motifs used in the dataset generation: The “house” motif (a) and its variant (b), and motif pairs with 1-WL indistinguishable nodes (c,d).

of subgraph motifs to Barabási-Albert random graph, the GNNExplainer reference implementation [30] performed better. This could be attributed to the fine-tuned denoising step and other domain specific architectural nuances in the reference implementation that were adapted for a better performance on the house dataset and its derivatives. For all other datasets, a standard out-of-the-box combination of GCN + GNNExplainer from the open source PyG [13] library was sufficient to yield very high accuracy. We used Glasgow Subgraph Solver [21], a high-performance subgraph isomorphism solver, for deciding rooted subgraph isomorphism. Most of the experiments were run on a machine(s) with the following architecture: **processor**: 72 cores of Intel(R) Xeon(R) Gold 6240 CPU @ 2.60GHz, **memory**: 392G, **graphics processor**: Nvidia Tesla V100-PCI-E-32GB.

Runtime Analysis On the largest graphs in the experiments with nearly 1,000 nodes, EEGL spent an average of 17 min. (1,044.66 sec.) for one iteration and for a single fold, with the following distribution among the modules (also in percentage): 11.54 sec. (1.1%) on the learning, 444.75 sec. (42.6%) on the explainer, 456.07 sec. (43.6%) on the pattern extraction, and 132.30 sec. (12.7%) on the feature annotation modules. Since EEGL computes everything from scratch in each iteration, the runtime grows *linearly* with K (number of iterations in Alg. 1). We note that EEGL was faster on all other graphs used in the experiments.

4.2 Graphs with Low 1-WL Symmetry

In this section we study the questions formulated in Sect. 1 for graphs for which all 1-WL classes contain relatively few elements only, compared to the graphs’ size. Since nodes belonging to different 1-WL classes are 1-WL distinguishable, such graphs have *low* 1-WL symmetry. They have *no* 1-WL symmetry if all 1-WL classes are singletons. In addition to this property, for all target classes c , the set of nodes in c is formed by the union of a family of 1-WL classes. For the experiments, we adopt the synthetic model of random graphs with motifs attached. This model, introduced in [30], has become a standard benchmark for GNN.

Datasets Graphs considered in this section are constructed as follows: Generate a Barabási-Albert (BA) random base graph [7] and attach copies of small graph motifs to m random nodes. The motifs are shown in Fig. 1, together with specifying how to attach them to the BA graph. For all motifs we used the same node and motif numbers as in [30], i.e., $n = 300$ and $m = 80$. For M_2 and M_2' , select one of the two motifs uniformly at random for each of the m copies and assign then the class labels to the nodes. The class labels of the motifs’ nodes are indicated in Fig. 1 and the nodes of the BA graph are all labeled by 0, except for the node with label 4 for M_1' . Finally, add a small amount of *structural noise* to the motifs via a small set of random edges. The graphs obtained in this way for M_1, \dots, M_2' in Fig. 1 are denoted by $G(M_1), \dots, G(M_2')$, respectively.

Note that for each motif M in Fig. 1, all nodes of $G(M)$ with label ℓ can be distinguished from the nodes with label ℓ' by some characteristic rooted pattern(s), for all $\ell > \ell' > 0$. For the nodes with label 0, we are not aware of a small set of such characteristic patterns. Class 0 is handled in the same way as all other classes.

The following considerations motivated our choice of the motifs. Regarding M_1 (Fig. 1a) used in GNNEXPLAINER [30], the three labels indicate its 1-WL classes. Its attachment to the base graph *breaks*, however, the 1-WL symmetry. In fact, $G(M_1)$ in the experiments had *no* 1-WL symmetry (i.e., all of its 1-WL classes were singletons). The only difference between $G(M_1')$ (see Fig. 1b for M_1') and $G(M_1)$ is that the base graph’s nodes are split into two classes by assigning label 4 to the attachment nodes. This kind of “merged” node classes are more challenging for vanilla GNNs. For both of the last two motif pairs in Fig. 1 we have that certain nodes within a pair are indistinguishable by 1-WL (e.g., the nodes with label 3 from those with label 6 in M_2 in Fig. 1c) and hence by vanilla GNNs as well. For $G(M_2)$ and $G(M_2')$, however, all base graph nodes belonged to a singleton 1-WL class and all motif nodes within a 1-WL class had the same class label and were in the same motif occurrence.

Experimental Results and Analysis The results are presented in Table 1. The rows correspond to the feature matrix definitions in GNN (LE, A, R), SHADOW-GNN [31], vanilla GNN (R0), and the first iteration of EEGL (R1). We used 10-fold CV and report the mean weighted F1-scores (percentage), together with the standard deviations. As

	$G(M_1)$	$G(M'_1)$	$G(M_2)$	$G(M'_2)$
Label Encoded (LE)	100.00±0.00	100.00±0.00	99.58±0.51	99.89±0.34
Adversarial (A)	97.71±1.14	80.50±4.59	79.45±4.39	71.51±5.95
Random (R)	96.38±2.46	93.23±3.79	95.62±4.44	79.57±3.98
SHADOW-GNN	100.00±0.00	96.29±4.89	73.09±7.07	87.65±9.00
EEGL Round-0 (R0)	98.56±1.83	90.82±4.12	61.53±3.39	56.81±3.40
EEGL Round-1 (R1)	99.86±0.42	99.29±0.71	99.45±0.55	99.36±0.69

Table 1: Average weighted F1-score results in percentage (mean ± SD) obtained with 10-fold CV for the motifs in Fig. 1 with the label encoding (LE), adversarial (A), random (R) settings, SHADOW-GNN, vanilla GNN (R0), and rounds 1 of EEGL (R1).

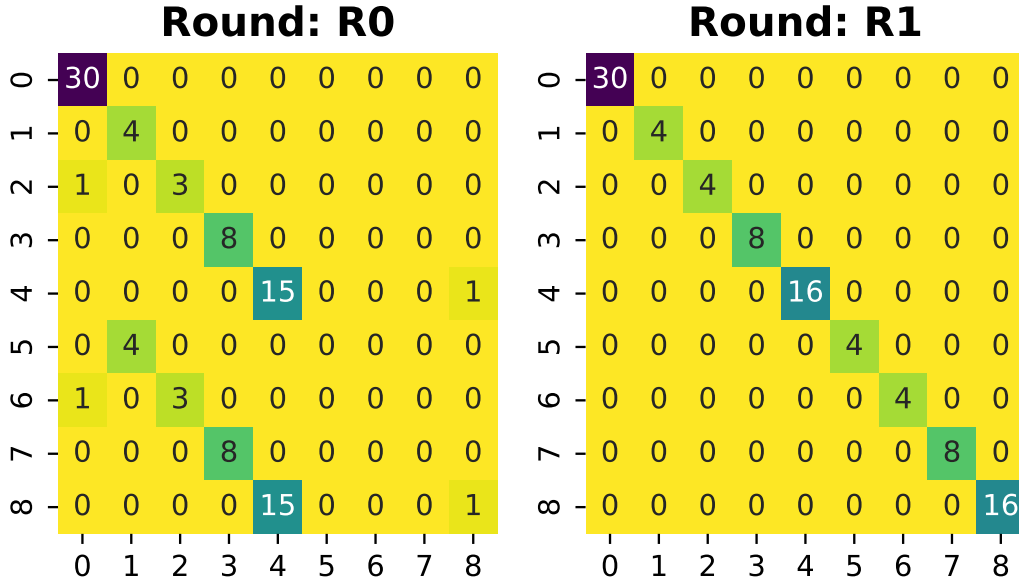


Figure 2: Example of the confusion matrices for a fold of $G(M'_2)$.

expected, GNN with the label encoding setting (LE) consistently achieved a result close to 100%. Thus, values in row LE should be regarded as *upper bounds* on performance achievable by GNN. Below we answer the questions formulated in Sect. 1 for graphs with low 1-WL symmetry. The quantitative experimental results are accompanied with an *analysis*. We peek under the hood of EEGL to understand its *training dynamics*.

Answer to Q1 We answer this question by comparing the results with vanilla GNN (R0) to those with EEGL’s first iteration (R1) (see Table 1). The order of the graphs in Table 1 follows their difficulty for vanilla GNN. While the results are inconclusive for $G(M_1)$ (R0 and R1 are both close to 100%), there is an improvement for all other graphs. In particular, EEGL achieved in one iteration a considerable improvement of around 38% and 43% on $G(M_2)$ and $G(M'_2)$, respectively. For example, out of the 94 test nodes, vanilla GNN (R0) classified only 61 correctly (see the confusion matrices in Fig. 2 for the test examples for one of the 10 folds for $G(M'_2)$). The number of correctly classified nodes increases to 94 (100%) in one round of EEGL (R1). This and other results of this section indicate that *EEGL is capable of iterative self-improvement from explanations already in one iteration*, giving an affirmative answer to Q1.

Answer to Q2 As noted earlier, LE (label encoding) provides an *upper bound* for achievable prediction, and it achieved almost perfect prediction for each variant. The “adversarial” (A) feature initialization addresses the issue that any set of subgraph features is expected to improve upon the prediction performance of GNN [8]. Comparing the improvement of EEGL with other feature initializations seems to be nontrivial. One possibility would be to consider random subgraph features, but it is not clear what would be the relevant notion of a random graph here. We consider a weakest possible formulation, and try to show that EEGL brings more improvement than some arbitrary feature initialization. This, however, includes cases when the subgraph features do not occur at all, and thus feature initialization trivializes. Therefore we attempt to find an “unhelpful” but nontrivial subgraph initialization. The approach is to use subgraph features which do not occur in the motifs, but may occur in the base graph. As the base graph is random, the features are expected to be of limited help. Note that motif nodes get a trivial initialization, but the nontrivial initialization of the base graph nodes may have an effect on them. Similarly to EEGL, these features are problem dependent as well. The experiments show that indeed, *EEGL (R1) is better than A* (see Table 1). Randomized feature initialization has

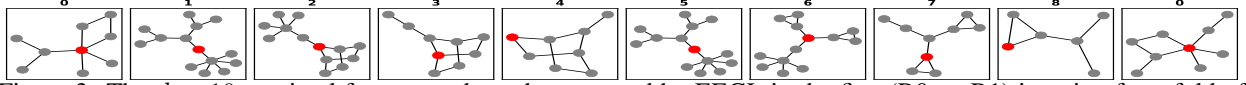


Figure 3: The $d = 10$ maximal frequent subgraphs extracted by EEGL in the first ($R0 \rightarrow R1$) iteration for a fold of $G(M'_2)$. Class labels indicated on top. There are two patterns for label 0.

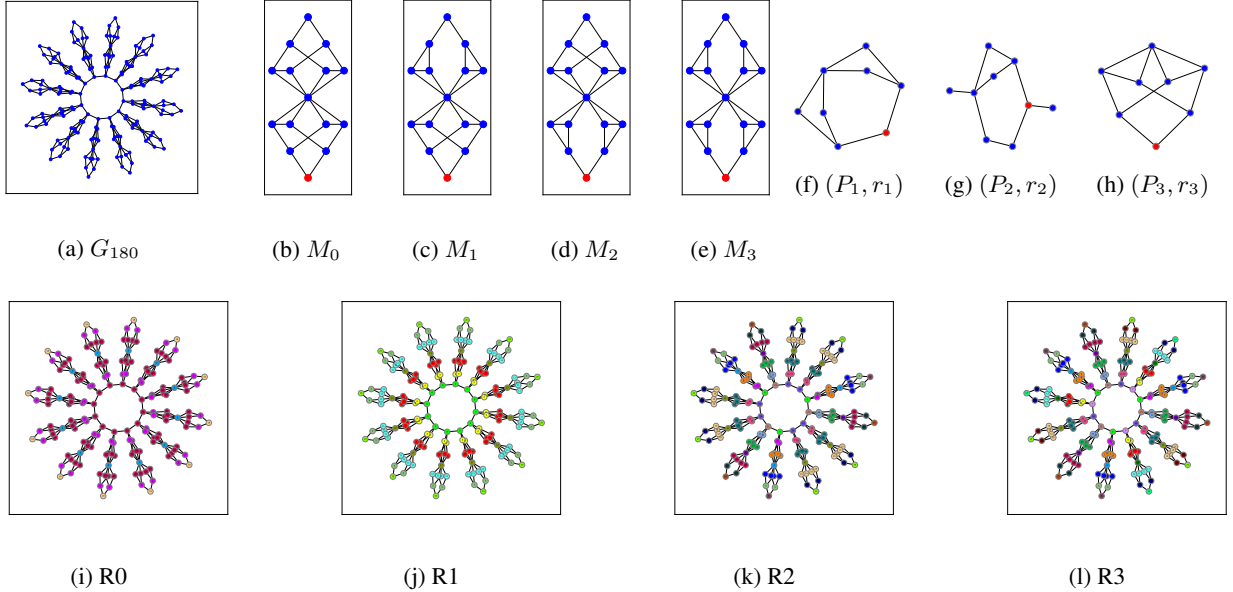


Figure 4: Graph G_{180} (a) obtained by attaching the four motifs in (b)–(e) via their bottom nodes (color red) in a rotating manner to the cycle of length 12 in the middle. The 28 target classes, denoted by the colors, are defined by the orbits. Top frequent patterns extracted by EEGL from the explanations in rounds 2 (f and g) and 3 (h) for G_{180} in Fig. 4a with their roots r_1, r_2, r_3 marked by red. The class predictions obtained by EEGL with vanilla initialization is given in (i)–(l). Each of the 28 colors denotes the same class in (i)–(l).

been shown to be powerful in a theoretical sense [1, 10]. Randomization extends GNNs in a different direction than EEGL. The comparison shows that *EEGL (R1) outperforms randomization (R)* already in one iteration on all graphs. Finally, while the difference between EEGL (R1) and SHADOW-GNN [31] is negligible on $G(M_1)$ and $G(M'_1)$, EEGL performs much better on $G(M_2)$ and $G(M'_2)$. In summary, the results on synthetic graphs with low 1-WL symmetry show that *EEGL outperforms other node feature definitions and SHADOW-GNN in predictive performance* already in one iteration, giving an affirmative answer to Q2 for this kind of graphs.

Answer to Q3 Consider again M'_2 (Fig. 1d) and the confusion matrices in Fig. 2 (see Appendix E for the detailed results on $G(M'_2)$). Prediction mistakes made by vanilla GNN (R0) indicates that it is sometimes unable to distinguish nodes belonging to different 1-WL classes in $G(M'_2)$, but to the same one locally, i.e., in M'_2 . As an example, for the nodes in the 1-WL indistinguishable classes 4 and 8 (cf. Fig. 1d) vanilla GNN predicts 1 node of class 4 by class 8 and conversely, 15 nodes of class 8 by 4. Out of 33 mistakes, 31 are of this type; the remaining two arise from classifying motif nodes with label 0. The picture for the first iteration of EEGL is different (see R1 in Fig. 2). Consider, for example, the label pair 4–8. The top 10 frequent patterns extracted in round 0 are given in Fig. 3 (same fold as in Fig. 2). One can check that the patterns for labels 4 and 8 are genuine in the sense that they distinguish nodes in these classes. The situation for label pairs 2–6 and 3–7 is similar. This is, however, not the case for 1–5. Still, EEGL (R1) can correct all mistakes on nodes of class 5. We speculate that this is because the neighbors of the nodes of the two classes have different feature vectors. In summary, our answer to Q3 is that the results suggest that *EEGL has an excellent performance on learning over graphs having low 1-WL symmetry and target classes are defined by unions of 1-WL classes*.

LE	100.00±0.00	
SHADOW-GNN	35.56±6.95	
EEGL	vanilla	random
R0	10.00±0.00	79.78±6.57
R1	56.96±34.70	99.26±1.48
R2	97.78±2.96	100±0.00
R3	100.00±0.00	100.0±0.0

Table 2: Average weighted F1-score results with SD in percentage obtained for G_{180} with 5-fold CV with the label encoding (LE) setting, with SHADOW-GNN [31], vanilla and random initialization (R0), and for three iterations of EEGL (R1, R2, R3).

4.3 Graphs with High 1-WL Symmetry

In this section we study a graph of type (ii) in Section 1, the case opposite to the one in Sect. 4.2. That is, the graph has a few 1-WL classes compared to its size, i.e., it has *high* 1-WL symmetry, and the equivalence relation defined by the target classes is a refinement of that induced by 1-WL.

Dataset The graph G_{180} , given in Fig. 4a, has 180 nodes and is obtained by attaching the four motifs in Figs. 4b–4e via their bottom nodes (red) to a cycle of length 12, denoted by C_{12} (see the middle of Fig. 4a). More precisely, denoting the nodes of C_{12} by v_0, \dots, v_{11} , v_i is the bottom node of a copy of motif M_k for $i \equiv k \pmod{4}$, for every $i = 0, \dots, 11$. There is no rooted isomorphism between any two motifs in Figs. 4b–4e mapping their bottom (i.e., red) nodes to each other. As a result, G_{180} has 28 orbits, denoted by the colors in Fig. 4l. These are the target classes. Two nodes of G_{180} belong to the same 1-WL class iff they have the same distance from C_{12} . Thus, the target classes define a proper refinement of the 1-WL classes.

Experimental Results and Analysis The mean weighted F1-score results with standard deviations obtained for G_{180} by 5-fold cross-validation with SHADOW-GNN [31] and with three iterations of EEGL (R1–R3) are given in Table 2. For EEGL we present the results for vanilla and for random feature initialization (R0). The parameter values were chosen with hyperparameter grid search. EEGL achieved an F1-score of 100% with both vanilla and random initialization, considerably outperforming SHADOW-GNN. Note also that the difference between vanilla and random GNN (R0) is nearly 70%. We speculate that this is due to the high 1-WL symmetry of G_{180} and the relationship between the 1-WL and the target classes.

In contrast to the graphs in Section 4.2, EEGL needed more than one iteration to achieve an F1-score of 100% on G_{180} . A closer look at the confusion matrices indicates that the difficulty is that each of the seven 1-WL equivalence classes is the union of four target classes. We illustrate the *training dynamics* of (vanilla) EEGL on one of the folds. In particular, for each iteration of EEGL we analyse the confusion matrix summarizing EEGL’s predictions for *all* 180 nodes (i.e., for the training examples as well) and present some extracted top frequent patterns to demonstrate how EEGL goes far beyond the node distinguishing power of 1-WL and hence, that of (vanilla) GNN.

Fig. 4i shows the result obtained with vanilla GNN (R0). The four colors indicate the four predicted classes. Comparing the predictions with the true class values in Fig. 4l, one can see that vanilla GNN achieves poor predictive performance. Somewhat surprisingly, it is even worse than that of 1-WL: While the nodes with distance 0, 2, and 4 from C_{12} are 1-WL distinguishable, vanilla GNN cannot distinguish among them. We note that the target classes are colored consistently in all graphs in Figs. 4i–4l. There is a similar problem with the nodes with distance 1 and 5 from C_{12} . Furthermore, all nodes e.g. of distance 6 from C_{12} are misclassified in R0. All top frequent patterns extracted from the local explanations in R0 are star graphs, with roots formed by their center nodes. Since patterns are matched with rooted subgraph isomorphism, these patterns define lower bound constraints on the nodes’ degree. Still, already these “weak” patterns suffice to improve the predictive performance in the first iteration R1 (see Fig. 4j). In fact, the class predictions obtained in R1 coincide with the 1-WL node partitioning. The top frequent patterns extracted from the local explanations in this round were semantically more meaningful, compared to those in R0. As an example, consider the rooted pattern (P_1, r_1) in Fig. 4f. While for any node v of G_{180} with distance 0 or 6 from C_{12} , there is a rooted subgraph isomorphism from (P_1, r_1) to (G_{128}, v) , such a rooted subgraph isomorphism does not exist e.g. for the nodes with distance 5 from C_{12} . On the other hand, from (P_2, r_2) in Fig. 4g there is a (resp. there is no) rooted subgraph isomorphism to (G_{128}, v) for all nodes v with distance 0 (resp. 6) from C_{12} . Thus, the combination of these two patterns can distinguish the nodes on C_{12} from those with distance 6 from C_{12} . Using the top frequent patterns extracted in R1 for feature annotation, a much better prediction is obtained in R2 (see Fig. 4k). In particular, all nodes belonging to a copy of M_0 (Fig. 4b) or M_3 (Fig. 4e) are correctly classified. Note that these two motifs are non-isomorphic to each other as well as to M_1 and M_2 . The nodes of M_1 (Fig. 4c) and M_2 (Fig. 4d) are, however, incorrectly classified. Though they are isomorphic motifs, there is no isomorphism between them mapping the bottom nodes (i.e., which lie on C_{12}) to each other. For the four occurrences of M_1 and for those of M_2 it holds that their nodes with the same distance from C_{12} are predicted with the same target class. Recall that they are 1-WL indistinguishable. Still, a combination of the top frequent patterns extracted in R2 is able to overcome this problem in the

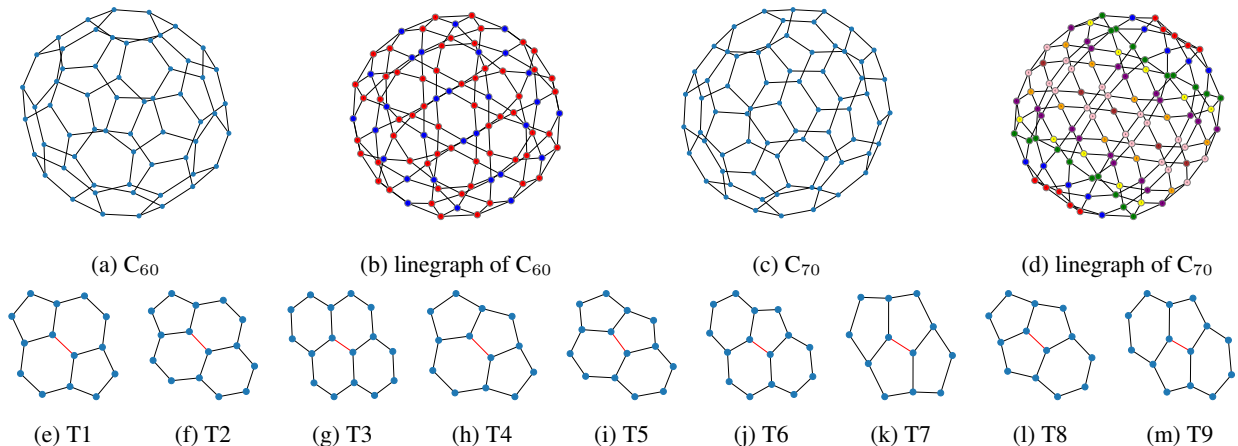


Figure 5: Fullerenes C_{60} (a) and its linegraph (b), C_{70} (c), and its line graph (d). The colors in (b) and (d) indicate the corresponding bond types in (a) and (c), respectively. The different [6,6], [5,6], and [5,5] types of the bonds (in red) are given in (e)–(m).

next iteration R3, obtaining the correct classification (Fig. 4l). As an example, one can check that the nodes of M_1 and M_2 with distance 6 from C_{12} in G_{128} become distinguishable by the rooted pattern in Fig. 4h. The example shows that it is possible for the predicted class to be incorrect for *all* nodes of a block (see, e.g., the nodes on C_{12} in Fig. 4i). Furthermore, while a block can remain unchanged after an iteration, its associated class may change (see, e.g., the nodes with distance 6 from C_{12} in Figs. 4i and 4j). In all such cases in the example considered, the new predicted class improves the accuracy.

Answers to Q1–Q3 In summary, for graphs that have high 1-WL symmetry and their 1-WL classes are formed by unions of target classes, the following are answers to the questions in Sect. 1. Regarding Q1, *EEGL is capable of iterative self-improvement from explanations*, but, unlike the graphs in Sect. 4.2, it needs more iterations. For Q2, *feature initializations may affect the number of iterations*. Running EEGL with random initialization required less iterations than vanilla. Also, *EEGL considerably outperformed SHADOW-GNN in predictive performance*. Finally, regarding Q3, it can handle this kind of relationships between 1-WL classes and (target) label partitions as well, implying that *EEGL has a distinguishing power that goes beyond the limitations of vanilla GNNs*.

4.4 Fullerenes

Now we turn to *fullerenes*, a large class of molecules made of carbon atoms only, having an atom-bond (graph) structure consisting of pentagons and hexagons [19]. Examples are C_{60} (the Buckminsterfullerene or “buckyball”) and C_{70} (see Figs. 5a and 5c). For every even $n \geq 20$ except 22, fullerenes with n carbon atoms contain 12 pentagonal and $n/2 - 10$ hexagonal faces (e.g., C_{60} is made of 12 pentagons and 20 hexagons). Their molecular graphs are 3-regular.

We consider bond (edge) classification problems. Target classes are defined either by bond lengths or by 9 patterns (red edges in Figs. 5e–5l surrounded by different combinations of four polygons). Edge classification is reduced to node classification by considering the line graphs of the atom-bond structure. The *line graph* of a graph G is a graph G' such that each vertex of G' represents an edge of G and two nodes of G' are connected by an edge iff their corresponding edges in G share a common node (line graphs of C_{60} and C_{70} are in Figs. 5b and 5d). The line graphs of fullerenes are 4-regular. Thus fullerene node and edge classification problems are of type (iii) in Section 1 and vanilla 1-WL cannot be used. Therefore in this section we use EEGL with random initialization (see Section 4.2).

Experimental Results and Analysis The results for different fullerenes¹⁰ are given in Table 3. The results show that EEGL (R2) has a high predictive performance on fullerenes and significantly outperforms SHADOW-GNN [31]. Table 3 includes also C_{60} and C_{70} (see Figs. 5a and 5c). Of the 9 patterns in Fig. 5 only two (T1 and T6) occur in C_{60} . Edge partitions by these patterns coincides with that by the two bond lengths in C_{60} (cf. Fig. 5b). EEGL achieved perfect classification in one iteration (R1) on C_{60} . Interestingly, instead of T1 and T6, EEGL extracted two semantically correct, more compact rules distinguishing these two classes: An edge is incident to the node of a pentagon (cf. T1), resp., an edge lies on a pentagon (cf. T6). On C_{70} , EEGL achieved 100% in R2.

¹⁰<https://nanotube.msu.edu/fullerene/fullerene-isomers.html>

fullerene	SHADow-GNN	R0	R1	R2
C24-D6d	68.68±20.83	84.29±24.91	100.00±0.00	100.00±0.00
C38-C1-3	36.70±9.77	36.81±9.08	97.40±5.19	97.45±5.09
C50-D5h-1	63.30±5.73	72.46±18.14	100.00±0.00	100.00±0.00
C60-1h	57.08±4.76	92.06±4.54	100.00±0.00	100.00±0.00
C70-D5h	56.87±8.27	62.99±11.18	93.27±13.46	100.00±0.00
C72-D6d	59.24±5.33	71.97±18.57	100.00±0.00	100.00±0.00
C74-D3h	52.71±10.66	64.24±18.03	87.70±24.60	87.70±24.60
C76-D2	63.50±8.41	66.00±7.94	100.00±0.00	100.00±0.00
C78-D3-1	51.82±10.54	59.78±10.90	100.00±0.00	100.00±0.00
C80-D5d-1	56.35±8.79	78.01±9.99	100.00±0.00	100.00±0.00
C82-C2-1	57.02±10.31	66.67±4.08	100.00±0.00	100.00±0.00
C84-D2-1	61.80±11.90	72.19±15.93	86.23±27.55	86.23±27.55
C86-C1-1	55.29±7.50	53.30±13.40	100.00±0.00	100.00±0.00
C90-D5h-1	62.92±5.59	73.46±10.82	100.00±0.00	100.00±0.00
C94-C2-1	55.93±5.00	64.44±9.81	100.00±0.00	100.00±0.00
C96-D2-1	63.17±6.28	78.36±9.43	100.00±0.00	100.00±0.00
C98-C2-1	61.65±6.53	65.79±13.57	100.00±0.00	100.00±0.00

Table 3: Average weighted F1-score results with SD in percentage obtained for different fullerenes with 5-fold CV with SHADow-GNN [31] and random initialization (R0), and for two iterations of EEGL (R1, R2).

For C_{70} , we also considered classifying edges by their length. While the number of target classes defined by the 9 structural patterns is only 4, the edges are partitioned into 8 blocks according to their bond lengths (Fig. 5d). EEGL achieved an F1-score of 100% in one iteration. It is interesting that the patterns extracted for this problem had a much weaker distinguishing power than those obtained for C_{60} , still, this incomplete information was sufficient for GNN to learn a perfect model. This is an example of the possibility, mentioned in Section 1, of making progress based on weak explanation.

Answers to Q1–Q2 In summary, *EEGL is capable of self-improvement from explanations* in one iteration (Q1) and *significantly outperforms SHADow-GNN* on this kind of learning task as well (Q2).

5 Concluding Remarks

We introduced EEGL, an iterative XAI-based model improvement approach to extend MPNN using frequent subgraph mining of explanation subgraphs to obtain features for improving predictive performance. The approach produced encouraging initial results, and it poses many directions for further research.

As we focused on graph-theoretic structural aspects, we have not considered node feature explanations. In future work we will consider this extension. A general question is to consider explanations from restricted tractable classes. This can be achieved either in the explainer (by modifying the denoising procedure in the case of GNNExplainer), or in the frequent subgraph miner. Another general question, continuing the list from the introduction is the following.

Q4: Does improved prediction performance in the iterations imply improved explanation quality?

There are several metrics for evaluating GNN explanations [17]. The evaluation of explanations in XAI is a difficult issue, with results on the problematic nature of explanations produced (see, e.g. [2]). The lack of ground truth exacerbates the difficulties. Considering synthetic or real-world problems where ground truth is available may be useful, but [12] warns of possible pitfalls. Considering node feature explanations could also be useful in this context as well.

References

- [1] R. Abboud, İ. İ. Ceylan, M. Grohe, and T. Lukasiewicz. The surprising power of graph neural networks with random node initialization. In *Proceedings of the Thirtieth International Joint Conference on Artificial Intelligence, IJCAI 2021*, pages 2112–2118. ijcai.org, 2021.
- [2] J. Adebayo, J. Gilmer, M. Muelly, I. J. Goodfellow, M. Hardt, and B. Kim. Sanity checks for saliency maps. In *Advances in Neural Information Processing Systems 31: Annual Conference on Neural Information Processing Systems 2018, NeurIPS 2018*, pages 9525–9536, 2018.
- [3] C. Agarwal, O. Queen, H. Lakkaraju, and M. Zitnik. Evaluating explainability for graph neural networks. *Scientific Data*, 10:144, 2023.

- [4] C. Agarwal, M. Zitnik, and H. Lakkaraju. Probing GNN explainers: A rigorous theoretical and empirical analysis of GNN explanation methods. In International Conference on Artificial Intelligence and Statistics, AISTATS 2022, volume 151 of Proceedings of Machine Learning Research, pages 8969–8996. PMLR, 2022.
- [5] M. Al-Shedivat, A. Dubey, and E. P. Xing. The intriguing properties of model explanations. CoRR, abs/1801.09808, 2018.
- [6] S. Ali, T. Abuhmed, S. El-Sappagh, K. Muhammad, J. M. Alonso-Moral, R. Confalonieri, R. Guidotti, J. D. Ser, N. D. Rodríguez, and F. Herrera. Explainable artificial intelligence (XAI): what we know and what is left to attain trustworthy artificial intelligence. Inf. Fusion, 99:101805, 2023.
- [7] A.-L. Barabási and R. Albert. Emergence of scaling in random networks. Science, 286(5439):509–512, 1999.
- [8] P. Barceló, F. Geerts, J. Reutter, and M. Ryschkov. Graph Neural Networks with Local Graph Parameters. In M. Ranzato, A. Beygelzimer, Y. Dauphin, P. S. Liang, and J. W. Vaughan, editors, Advances in Neural Information Processing Systems, volume 34, pages 25280–25293. Curran Associates, Inc., 2021.
- [9] G. Bouritsas, F. Frasca, S. Zafeiriou, and M. M. Bronstein. Improving graph neural network expressivity via subgraph isomorphism counting. IEEE Trans. Pattern Anal. Mach. Intell., 45(1):657–668, 2023.
- [10] G. Dasoulas, L. D. Santos, K. Scaman, and A. Virmaux. Coloring graph neural networks for node disambiguation. In Proceedings of the Twenty-Ninth International Joint Conference on Artificial Intelligence, IJCAI 2020, pages 2126–2132. ijcai.org, 2020.
- [11] V. P. Dwivedi, C. K. Joshi, A. T. Luu, T. Laurent, Y. Bengio, and X. Bresson. Benchmarking graph neural networks. J. Mach. Learn. Res., 24:43:1–43:48, 2023.
- [12] L. Faber, A. K. Moghaddam, and R. Wattenhofer. When comparing to ground truth is wrong: On evaluating GNN explanation methods. In KDD '21: The 27th ACM SIGKDD Conference on Knowledge Discovery and Data Mining, pages 332–341. ACM, 2021.
- [13] M. Fey and J. E. Lenssen. Fast graph representation learning with PyTorch Geometric. In ICLR Workshop on Representation Learning on Graphs and Manifolds, 2019.
- [14] F. Friedrich, W. Stammer, P. Schramowski, and K. Kersting. A typology to explore and guide explanatory interactive machine learning. CoRR, abs/2203.03668, 2022.
- [15] F. Friedrich, W. Stammer, P. Schramowski, and K. Kersting. A typology for exploring the mitigation of shortcut behaviour. Nat. Mac. Intell., 5(3):319–330, 2023.
- [16] W. L. Hamilton, R. Ying, and J. Leskovec. Representation learning on graphs: Methods and applications. IEEE Data Engineering Bulletin, pages 52–74, 2017.
- [17] J. Kakkad, J. Jannu, K. Sharma, C. C. Aggarwal, and S. Medya. A survey on explainability of graph neural networks. CoRR, abs/2306.01958, 2023.
- [18] T. N. Kipf and M. Welling. Semi-supervised classification with graph convolutional networks. In International Conference on Learning Representations (ICLR), 2017.
- [19] X. Lu, T. Akasaka, and Z. Slanina. Handbook of Fullerene Science and Technology. Springer Singapore, 2022.
- [20] S. Maekawa, K. Noda, Y. Sasaki, and M. Onizuka. Beyond real-world benchmark datasets: An empirical study of node classification with GNNs. In NeurIPS, 2022.
- [21] C. McCreesh, P. Prosser, and J. Trimble. The glasgow subgraph solver: Using constraint programming to tackle hard subgraph isomorphism problem variants. In F. Gadducci and T. Kehrer, editors, Graph Transformation - 13th International Conference, ICGT 2020, Proceedings, volume 12150 of Lecture Notes in Computer Science, pages 316–324. Springer, 2020.
- [22] C. Morris, Y. Lipman, H. Maron, B. Rieck, N. M. Kriege, M. Grohe, M. Fey, and K. M. Borgwardt. Weisfeiler and Leman go machine learning: The story so far. CoRR, abs/2112.09992, 2021.
- [23] C. Morris, M. Ritzert, M. Fey, W. L. Hamilton, J. E. Lenssen, G. Rattan, and M. Grohe. Weisfeiler and Leman go neural: Higher-order graph neural networks. In The Thirty-Third AAAI Conference on Artificial Intelligence, AAAI 2019, pages 4602–4609. AAAI Press, 2019.
- [24] H. Naik and G. Turán. Explanation from specification. CoRR, abs/2012.07179, 2020.
- [25] S. Nijssen and J. N. Kok. A quickstart in frequent structure mining can make a difference. In Proc. of the Tenth ACM SIGKDD International Conference on Knowledge Discovery and Data Mining, pages 647–652. ACM, 2004.

- [26] S. Nijssen and J. N. Kok. The gaston tool for frequent subgraph mining. Electronic Notes in Theoretical Computer Science, 127(1):77–87, 2005. Proceedings of the International Workshop on Graph-Based Tools (GraBaTs 2004).
- [27] Q. Sun, J. Li, H. Peng, J. Wu, Y. Ning, P. S. Yu, and L. He. SUGAR: subgraph neural network with reinforcement pooling and self-supervised mutual information mechanism. In WWW '21: The Web Conference 2021, pages 2081–2091, 2021.
- [28] L. Weber, S. Lopuschkin, A. Binder, and W. Samek. Beyond explaining: Opportunities and challenges of XAI-based model improvement. Inf. Fusion, 92:154–176, 2023.
- [29] K. Xu, S. Jegelka, W. Hu, and J. Leskovec. How Powerful are Graph Neural Networks? In 7th International Conference on Learning Representations, ICLR 2019, pages 1–17, 2019.
- [30] Z. Ying, D. Bourgeois, J. You, M. Zitnik, and J. Leskovec. Gnnexplainer: Generating explanations for graph neural networks. In H. Wallach, H. Larochelle, A. Beygelzimer, F. d'Alché-Buc, E. Fox, and R. Garnett, editors, Advances in Neural Information Processing Systems, volume 32. Curran Associates, Inc., 2019.
- [31] H. Zeng, M. Zhang, Y. Xia, A. Srivastava, A. Malevich, R. Kannan, V. K. Prasanna, L. Jin, and R. Chen. Decoupling the depth and scope of graph neural networks. In Advances in Neural Information Processing Systems 34: Annual Conference on Neural Information Processing Systems 2021, NeurIPS 2021, pages 19665–19679, 2021.

Supplementary Materials for the Submission Titled

Iterative Graph Neural Network Enhancement via Frequent Subgraph Mining of Explanations

In Appendix A we collect the necessary background about graph neural networks, the GNNEXPLAINER system, and frequent connected subgraph mining. Appendix C gives a high-level pictorial representation of the EEGL framework. In Appendix D we describe the pattern-extraction module which is a pre-requisite step for the top-k pattern filtering and the annotation phases. In Appendix E we report the detailed experimental results obtained for M_2^l (Fig. 1e in the submission) for all 10 folds. After the review process is complete, the source code will be publicly shared on Github.

A Background

For necessary background on GNN, GNNEXPLAINER, the Weisfeiler-Leman algorithm, and frequent subgraph mining, the reader is referred to [16, 26, 30].

Graph Neural Networks (GNN) We give a simplified description of GNN, corresponding to the type of networks used in GNNEXPLAINER [30]. In this paper we consider node classification. A GNN model Φ has as its inputs a graph $G = (V, E)$ and a feature matrix $X \in \mathbb{R}^{d \times |V|}$, where $X_v \in \mathbb{R}^d$ is a d -dimensional feature vector associated for every node $v \in V$. It computes the representation z_v , the embedding of each node $v \in V$, via L layers of neural message passing as follows. Starting with initial node features $h_i^0 = X_{v_i}$ for every $v_i \in V$, repeat the following three steps for each layer $l \in [L]$:

- (i) Compute neural messages $m_{ij}^l = \text{MSG}(h_i^{l-1}, h_j^{l-1}, r_{ij})$ for every pair of nodes $(v_i, v_j) \in V$, where MSG is the function which computes the message passed from v_j to v_i , and r_{ij} is a relation between v_i and v_j , e.g., the edge relation. Usually the message is h_j^{l-1} if $(v_i, v_j) \in E$, else 0.
- (ii) For each node v_i aggregate the messages from its neighborhood \mathcal{N}_{v_i} as $M_i^l = \text{AGG}(m_{ij}^l | v_j \in \mathcal{N}_{v_i})$, where AGG is the function used to aggregate all the messages passed from the neighborhood. AGG should be invariant or equivariant to the permutations of its inputs.
- (iii) For every node v_i update its features for using the aggregated messages from the neighborhood and the previous features as $h_i^l = \text{UPDATE}(M_i^l, h_i^{l-1})$, where UPDATE is the function used to combine the two inputs.

After the computation through the L layers, the embedding for every node v_i is the features computed for the L 'th layer i.e. $z_{v_i} = h_i^L$. For a fully supervised node classification task, the training loss is $\mathcal{L} = \sum_{v \in \mathcal{V}_{train}} -\log(\text{softmax}(z_v, y_v))$, where $y_v \in \{0, 1\}^c$ is one-hot vector indicating the ground truth label for node v , c is number of labels, and \mathcal{V}_{train} is the set of nodes in the training set.

GNNEXPLAINER [30] was the first general model-agnostic approach specifically designed for post-hoc explanations on graph learning tasks. Given a graph G , and a query in the form of a node in the graph, it identifies a compact subgraph structure and a small subset of node features that show significant evidence in playing a role in the prediction of the query node. The GNNExplainer procedure accomplishes this by formulating the explanation generation problem as an optimization task that maximizes the mutual information between a GNN's prediction and subgraph structures.

Frequent Subgraph Mining Frequent subgraph mining, a well-established subfield of data mining, is concerned with the following problem: *Given* some finite (multi)set \mathcal{D} of graphs and a frequency threshold $\tau \in (0, 1]$, *generate* all *connected* graphs that are subgraphs of at least $\lceil \tau |\mathcal{D}| \rceil$ graphs in \mathcal{D} . In the EEGL system we use GASTON [26], one of the most popular algorithms for the generation of frequent connected subgraphs. Similarly to most other heuristics designed for frequent subgraph mining, GASTON is based on the generate-and-test paradigm. One of its distinguishing features compared to other frequent subgraph mining algorithms is that it enumerates frequent patterns in accordance with a structural hierarchy (path, trees, and cyclic graphs), where cyclic patterns are generated in a DFS manner, "refining" frequent patterns by extending them with some new edge. Regarding its pattern matching component, i.e., which decides whether a candidate pattern is frequent or not, GASTON utilizes that frequent patterns are generated in increasing size. Instead of testing subgraph isomorphism from scratch for the graphs in \mathcal{D} , it stores the embeddings of the frequent patterns already found and decides subgraph isomorphism for a candidate pattern by utilizing the embeddings calculated for its antecedents.

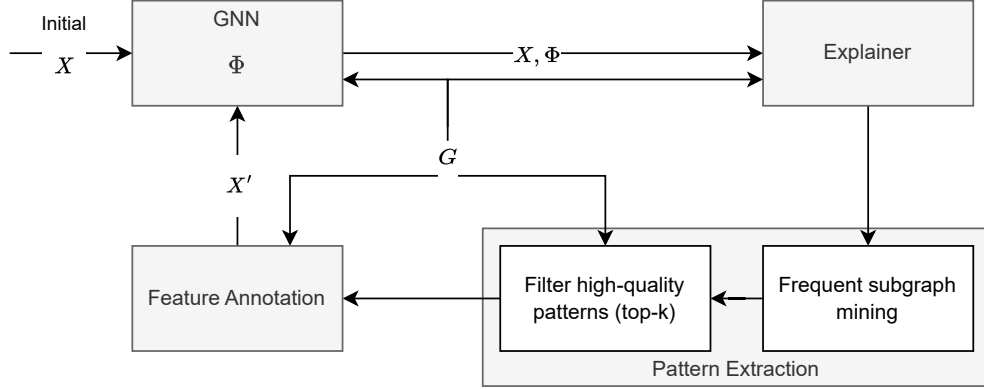


Figure 6: High-level depiction of the EEGL Process

B shadow-GNN

Regular GCN’s compute the node-features from a scope - which is a k -hop neighborhood of nodes - via a k -depth GCN. SHADOW-GNN [31] argues that this leads to oversmoothing of node-features, because mostly only a few nodes in the neighborhood of a node are relevant for the property/label of that node. This is especially worsened if the relevant nodes are somewhat farther in the graph, because then we need a large k to get them into the scope. Hence the entire k -hop neighborhood becomes too big a scope for computing node features, and it becomes hard to discern useful information from the few relevant nodes among too much noise from the sea of irrelevant nodes. They argue that the scope should only be a subgraph of the k -hop neighborhood, and the depth l of a GCN should be decoupled from the scope of a node. With this decoupling, SHADOW-GNN can have GCN’s with any depth over the reduced scope which should fix the oversmoothing of the node features. However this introduces a new problem of identifying a good scope for the nodes. They propose methods using random-walk, personalised page rank(PPR) etc. to filter the scope from the neighborhood.

C Explanation Enhanced Graph Learning

Figure 6 shows a high level abstraction of the four major phases of the EEGL framework. We also note that the pattern extraction module consists of two sub-modules 1. Frequent-subgraph mining 2. Top-k pattern filtering

D Pattern Extraction Module

For a class label $c \in C$, MAXIMAL_FREQUENT_PATTERN_MINING (line 9 of Alg. 1) computes a set of maximal frequent rooted patterns in \mathcal{E}_c in two steps: (i) It generates a set of frequent rooted subgraphs of \mathcal{E}_c and (ii) selects the maximal rooted patterns from this set.

Regarding (i), the following frequent pattern mining problem is solved: *Given* \mathcal{E}_c containing m explanation graphs for some $m \geq 0$ integer and a frequency threshold $\tau \in (0, 1]$, *enumerate* the set of rooted patterns (P, r) such that (P, r) is frequent, i.e., there is a set $\mathcal{E}'_c \subseteq \mathcal{E}_c$ of rooted explanation graphs such that $|\mathcal{E}'_c| = \lceil \tau m \rceil$ and for all $(P', r') \in \mathcal{E}'_c$ there exists a rooted subgraph isomorphism from (P, r) to (P', r') . Note that \mathcal{E}_c may contain explanation graphs that are not associated with a root. While such explanation graphs do not support any of the frequent rooted patterns, they have an impact on the rooted patterns’ (relative) frequencies. The above problem is solved by GASTON [25] as follows: For all rooted explanation graphs $(P, v) \in \mathcal{E}_c$, v is associated with a distinguished node attribute label. Running GASTON on these modified explanation graphs with frequency threshold τ , it returns a set of frequent subgraphs. From this set we keep only the connected components of the frequent subgraphs that contain a node with the distinguished attribute label. This node will be regarded as the root of the pattern.

Regarding (ii), we remove all rooted patterns returned in the previous step that have a rooted subgraph isomorphism to some other rooted pattern and return the remaining rooted pattern set.

E Results

In this section we present the detailed results obtained for M'_2 (Fig. 1e in the submission). For each of the 10 folds, we present the

- the weighted F1-score results in percentage (top left table) obtained with the label encoding, random, and adversarial settings, as well as after the three iterations of EEGL (Round-0, Round-1, Round-2),
- the frequencies of the node labels in the test data (top right table),
- the confusion matrices obtained with the label encoding, random, and adversarial settings, as well as after the three iterations of EEGL (Round-0, Round-1, Round-2),
- the $d = 10$ maximal frequent subgraphs extracted by EEGL in the first ($R0 \rightarrow R1$) and the second ($R1 \rightarrow R2$) iteration. (Class labels are indicated on the top. Note that we can have more than one pattern for a node label.)

Fold 01

	F1-Score
Label Encoded (LE)	100.00
Adversarial (A)	67.25
Random (R)	85.05
EEGL Round-0	54.94
EEGL Round-1	100.00

Table 4: F1-Scores for fold-01

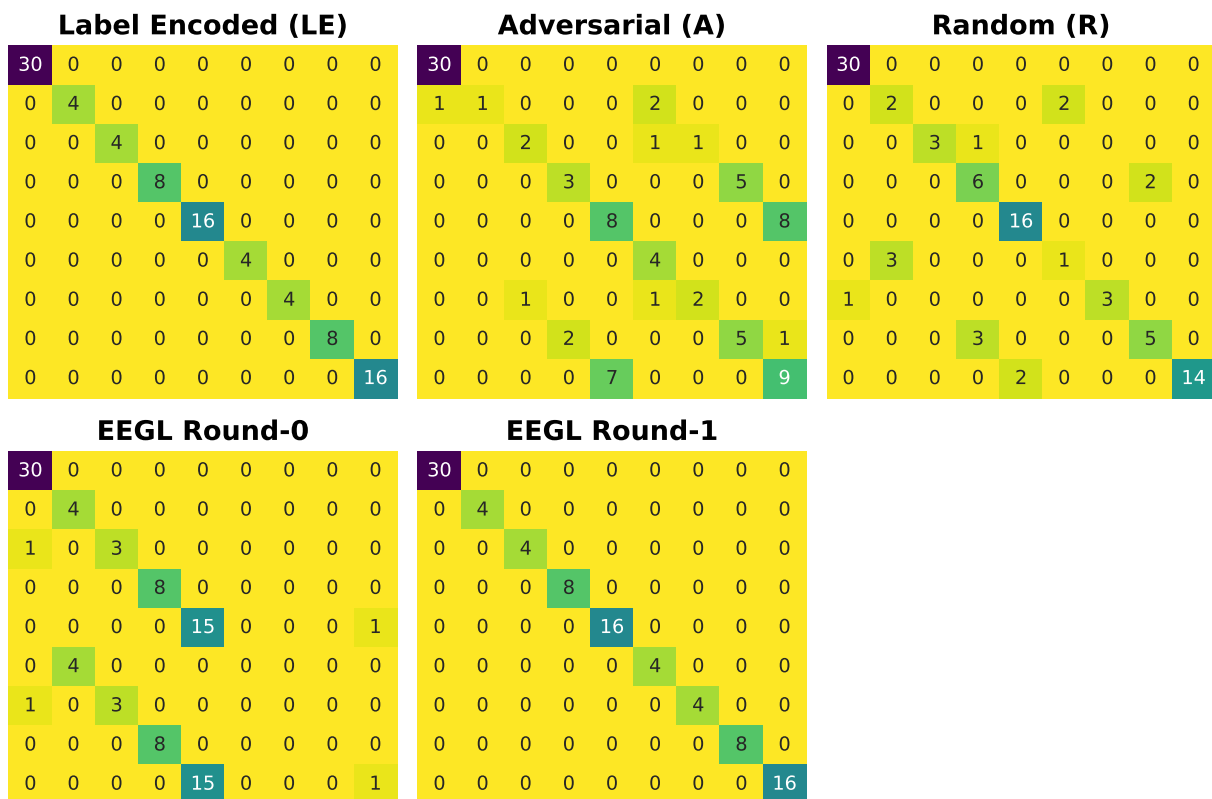
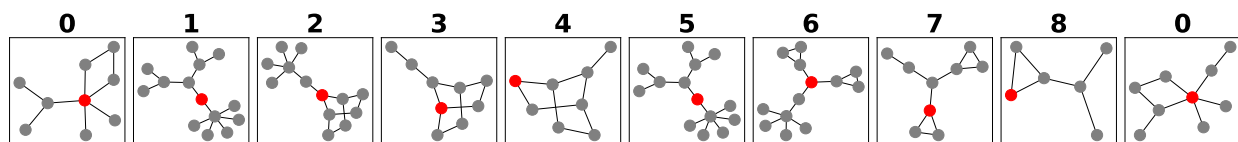


Figure 7: Confusion Matrix for fold-01


 Figure 8: Top-K patterns for fold-01 from round-0 explanations. These patterns were used to annotate features for round-1

Fold 02

	F1-Score
Label Encoded (LE)	100.00
Adversarial (A)	78.08
Random (R)	86.07
EEGL Round-0	60.55
EEGL Round-1	100.00

Table 5: F1-Scores for fold-02

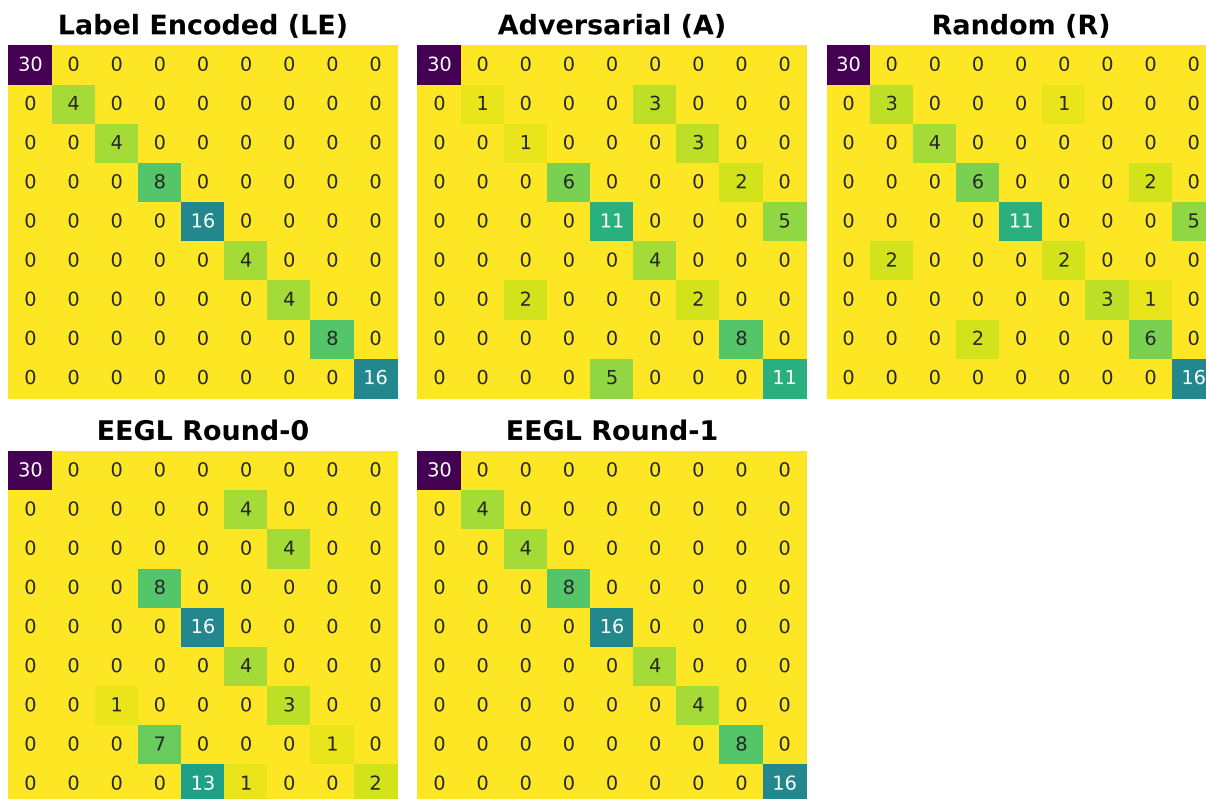
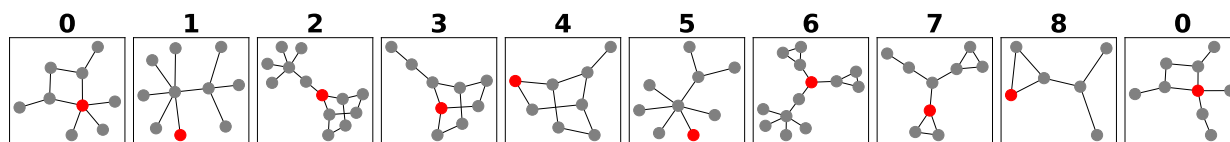


Figure 9: Confusion Matrix for fold-02


 Figure 10: Top-K patterns for fold-02 from round-0 explanations. These patterns were used to annotate features for round-1

Fold 03

	F1-Score
Label Encoded (LE)	100.00
Adversarial (A)	79.86
Random (R)	79.62
EEGL Round-0	54.25
EEGL Round-1	100.00

Table 6: F1-Scores for fold-03

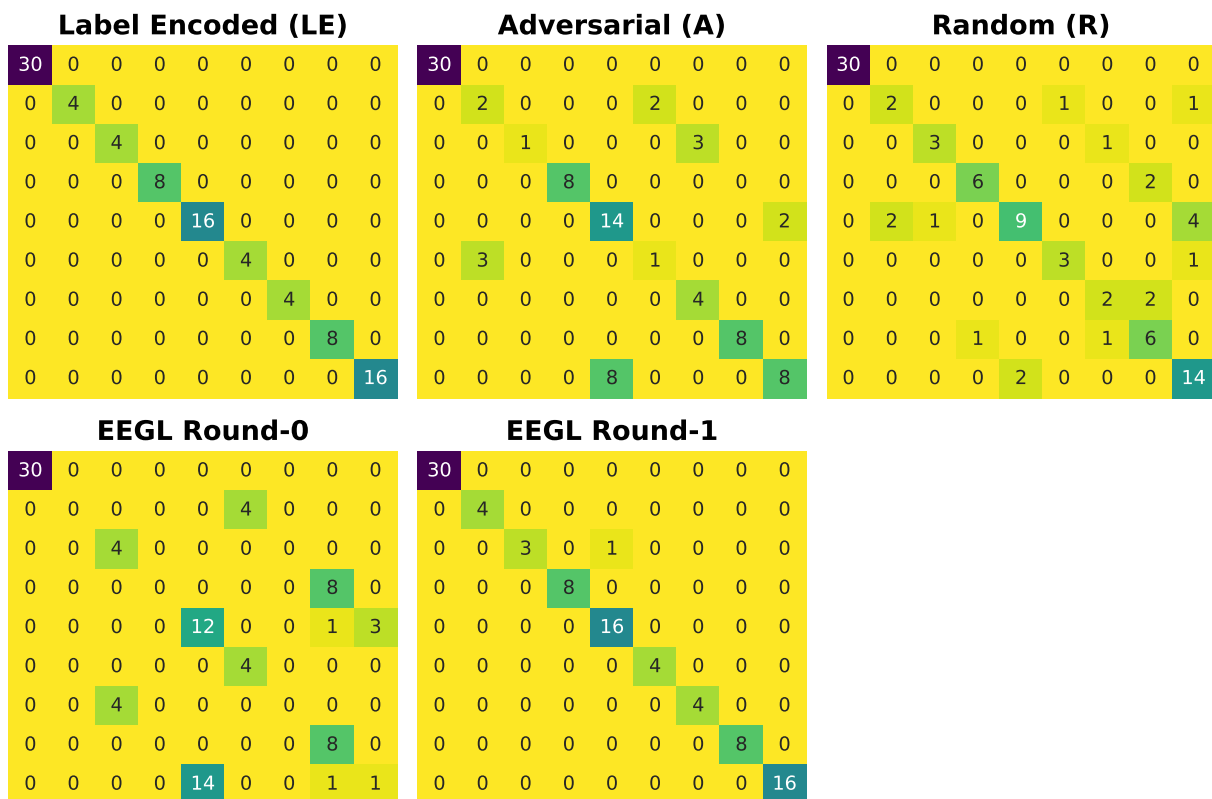
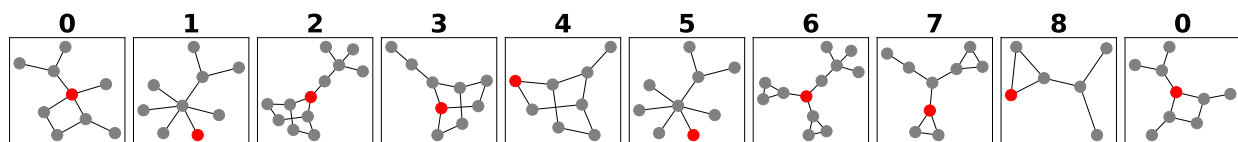


Figure 11: Confusion Matrix for fold-03


 Figure 12: Top-K patterns for fold-03 from round-0 explanations. These patterns were used to annotate features for round-1

Fold 04

	F1-Score
Label Encoded (LE)	100.00
Adversarial (A)	66.08
Random (R)	78.14
EEGL Round-0	50.90
EEGL Round-1	100.00

Table 7: F1-Scores for fold-04

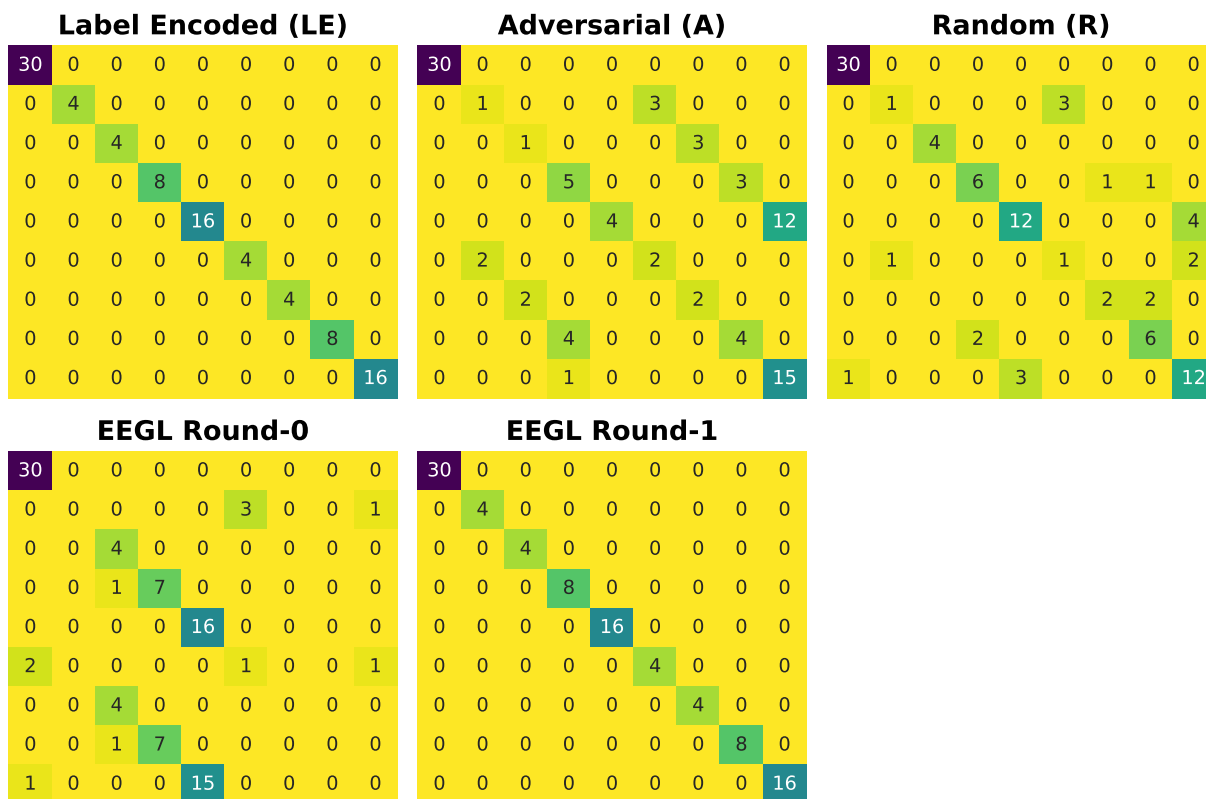
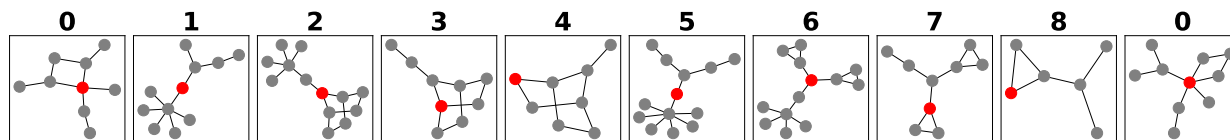


Figure 13: Confusion Matrix for fold-04


 Figure 14: Top-K patterns for fold-04 from round-0 explanations. These patterns were used to annotate features for round-1

Fold 05

	F1-Score
Label Encoded (LE)	100.00
Adversarial (A)	68.93
Random (R)	80.93
EEGL Round-0	60.18
EEGL Round-1	100.00

Table 8: F1-Scores for fold-05

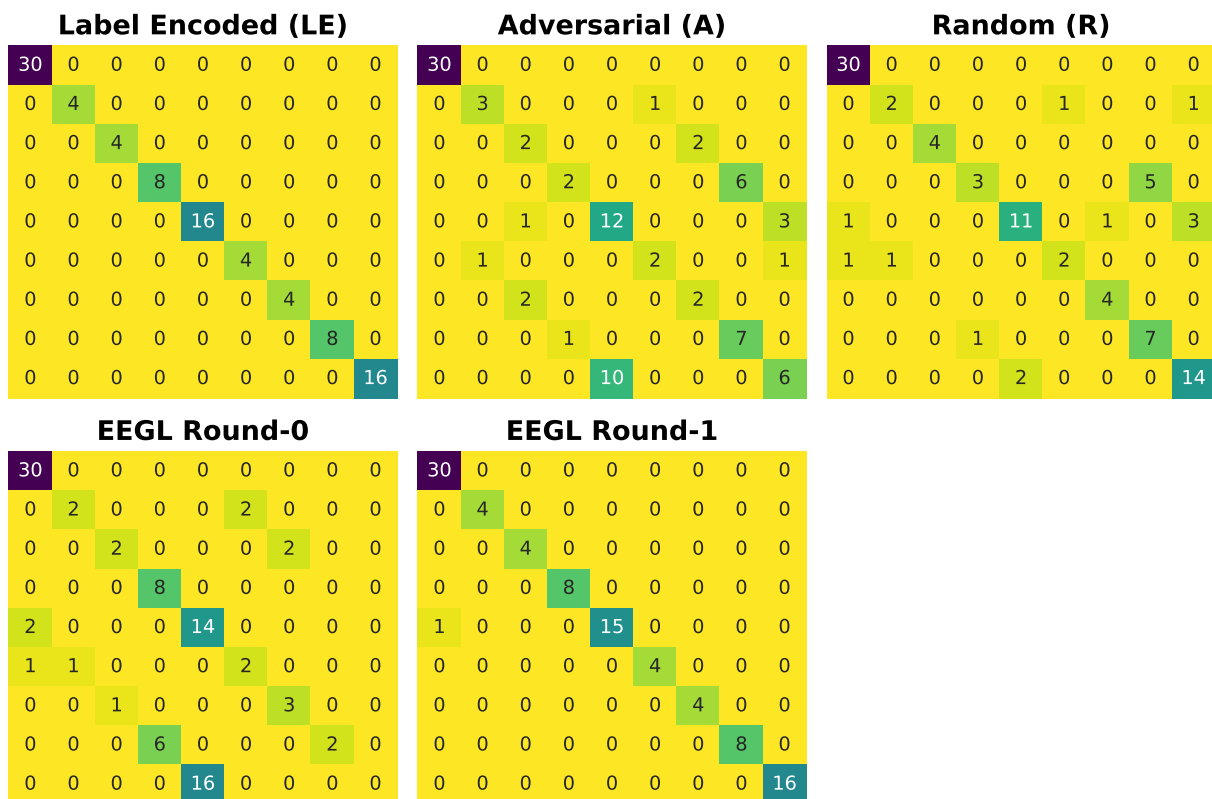
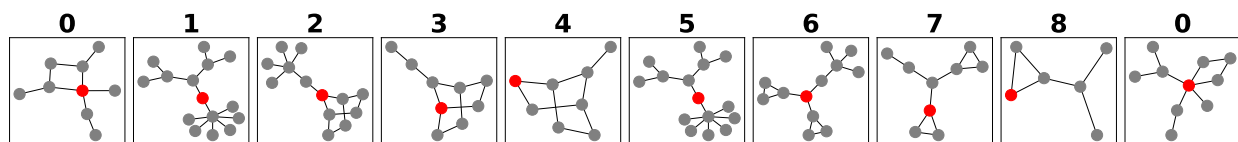


Figure 15: Confusion Matrix for fold-05


 Figure 16: Top-K patterns for fold-05 from round-0 explanations. These patterns were used to annotate features for round-1

Fold 06

	F1-Score
Label Encoded (LE)	100.00
Adversarial (A)	73.01
Random (R)	72.72
EEGL Round-0	59.71
EEGL Round-1	100.00

Table 9: F1-Scores for fold-06

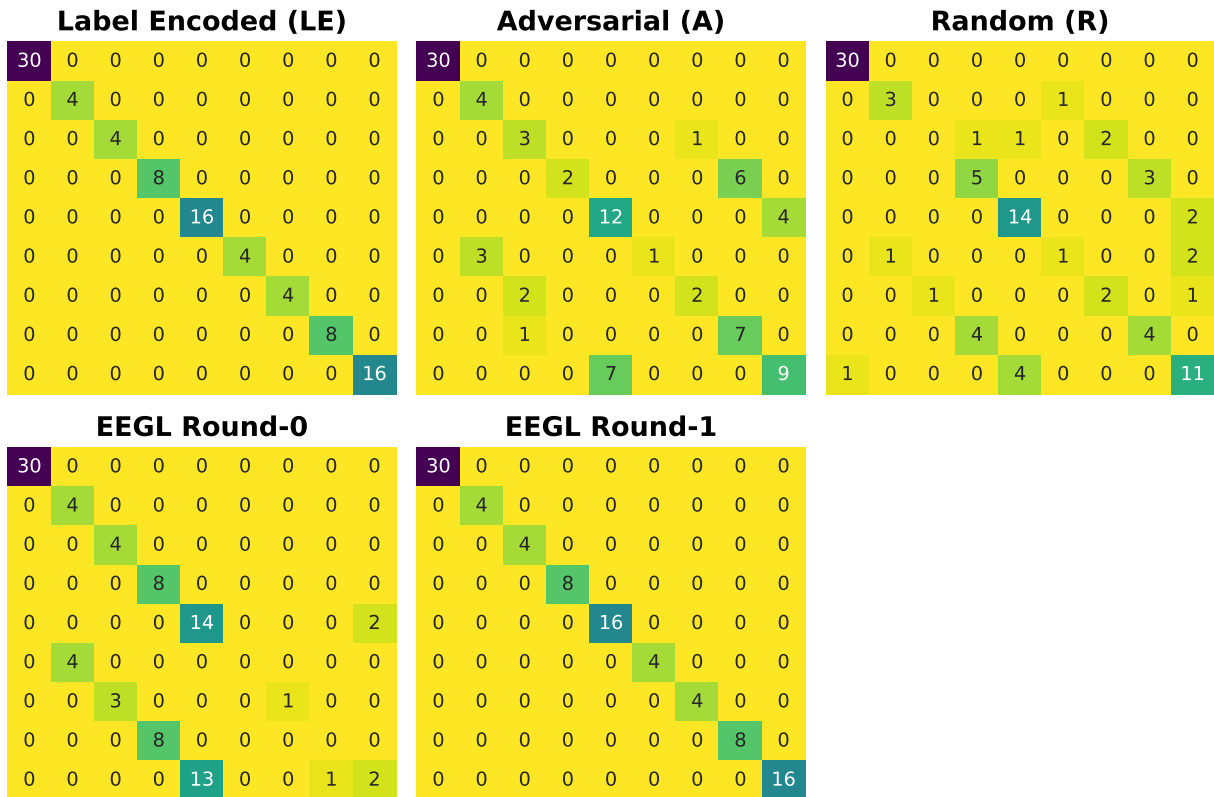


Figure 17: Confusion Matrix for fold-06

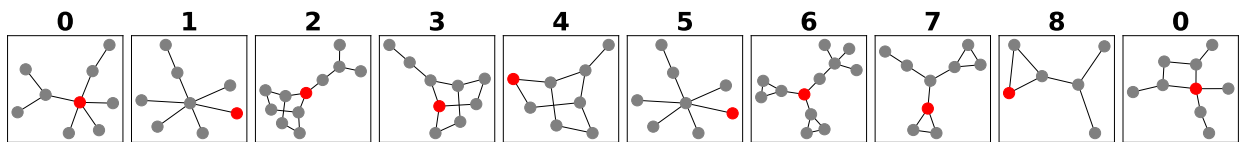


Figure 18: Top-K patterns for fold-06 from round-0 explanations. These patterns were used to annotate features for round-1

Fold 07

	F1-Score
Label Encoded (LE)	100.00
Adversarial (A)	73.01
Random (R)	72.72
EEGL Round-0	59.71
EEGL Round-1	100.00

Table 10: F1-Scores for fold-07

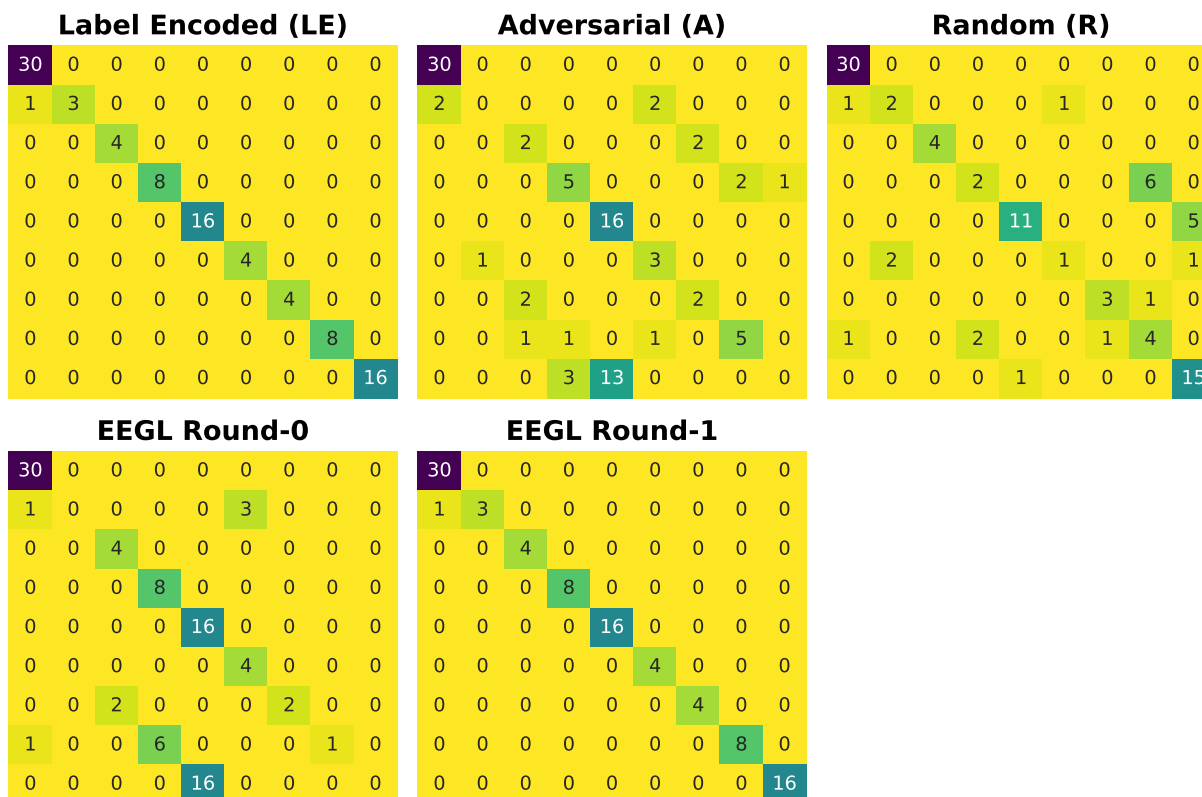
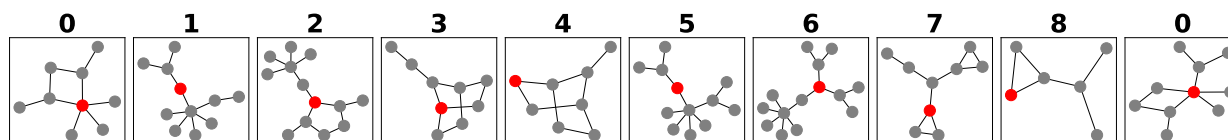


Figure 19: Confusion Matrix for fold-07


 Figure 20: Top-K patterns for fold-07 from round-0 explanations. These patterns were used to annotate features for round-1

Fold 08

	F1-Score
Label Encoded (LE)	100.00
Adversarial (A)	75.48
Random (R)	81.40
EEGL Round-0	54.54
EEGL Round-1	100.00

Table 11: F1-Scores for fold-08

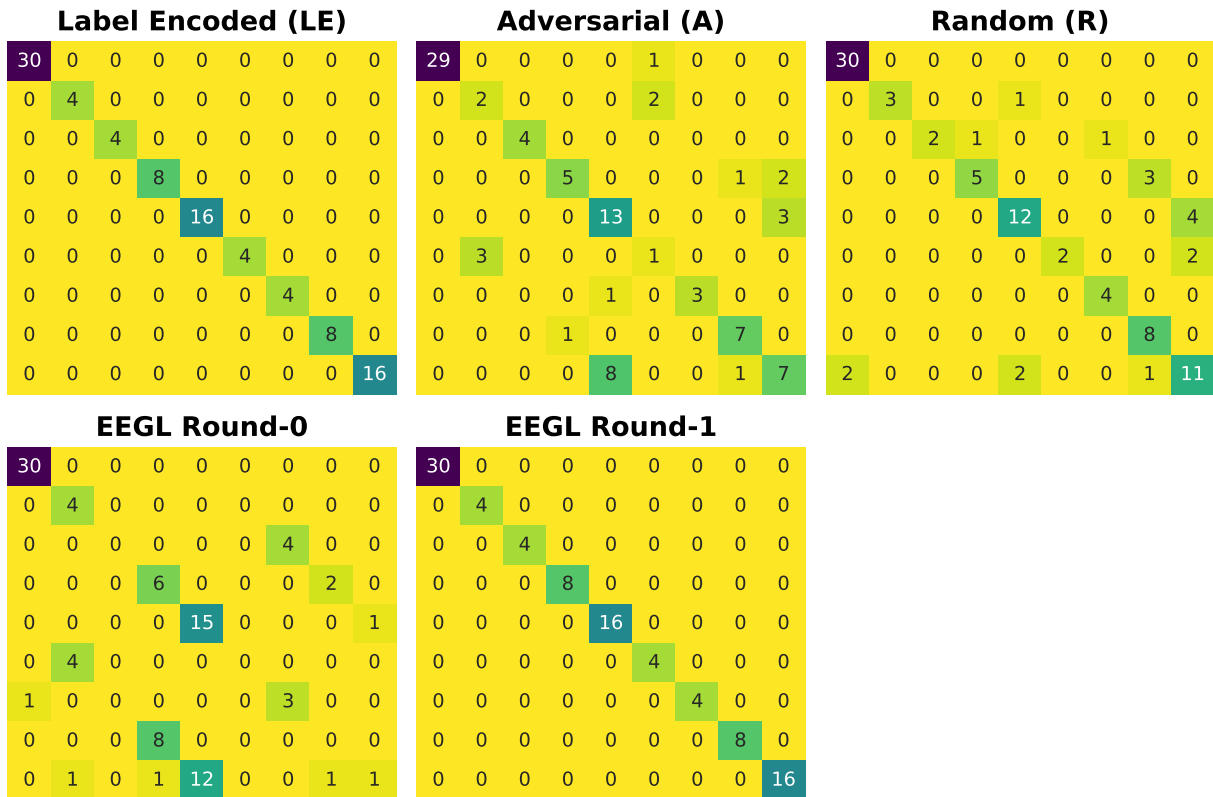


Figure 21: Confusion Matrix for fold-08

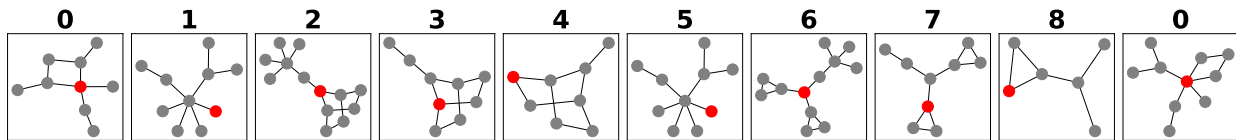


Figure 22: Top-K patterns for fold-08 from round-0 explanations. These patterns were used to annotate features for round-1

Fold 09

	F1-Score
Label Encoded (LE)	100.00
Adversarial (A)	77.39
Random (R)	80.46
EEGL Round-0	60.11
EEGL Round-1	98.01

Table 12: F1-Scores for fold-09

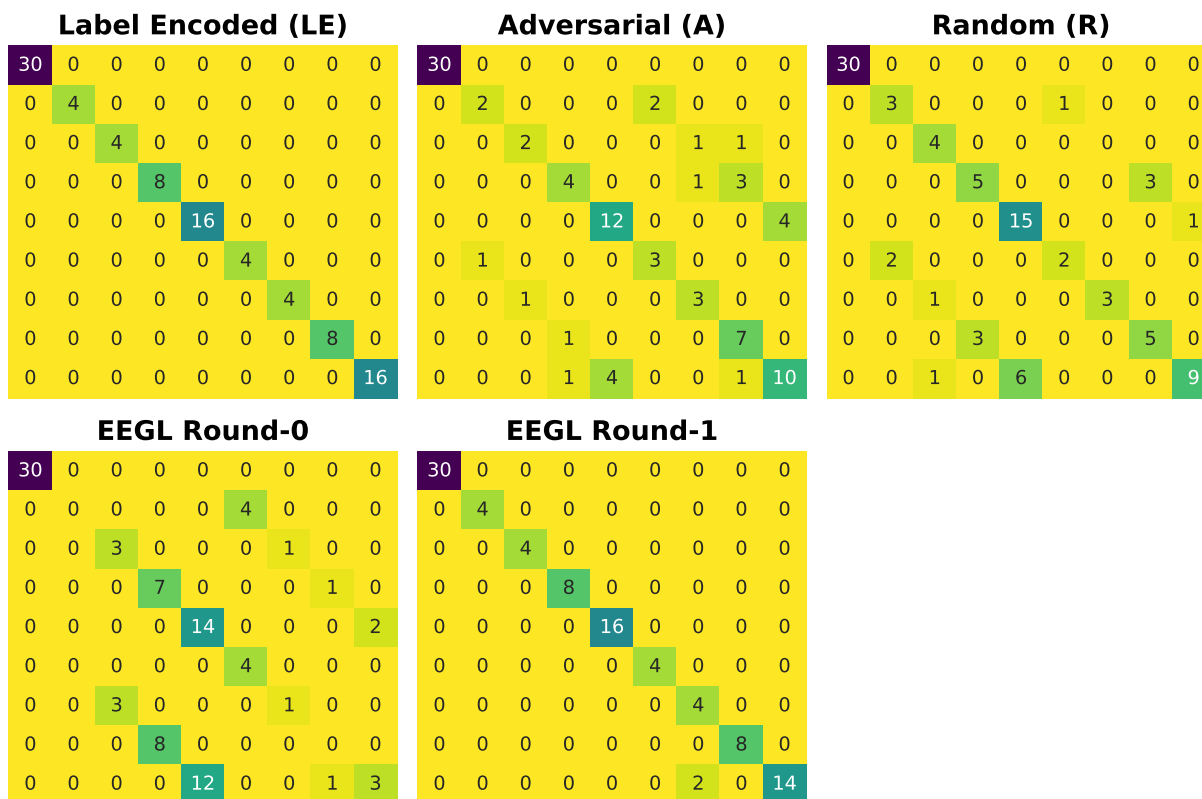
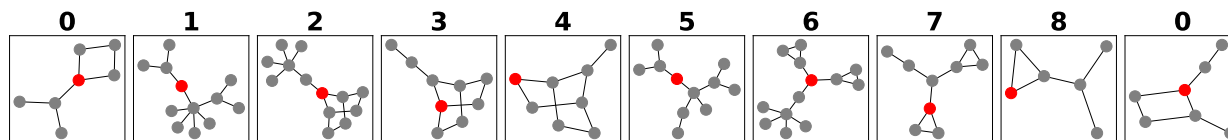


Figure 23: Confusion Matrix for fold-09


 Figure 24: Top-K patterns for fold-09 from round-0 explanations. These patterns were used to annotate features for round-1

Fold 10

	F1-Score
Label Encoded (LE)	100.00
Adversarial (A)	68.75
Random (R)	75.83
EEGL Round-0	53.28
EEGL Round-1	98.88

Table 13: F1-Scores for fold-10

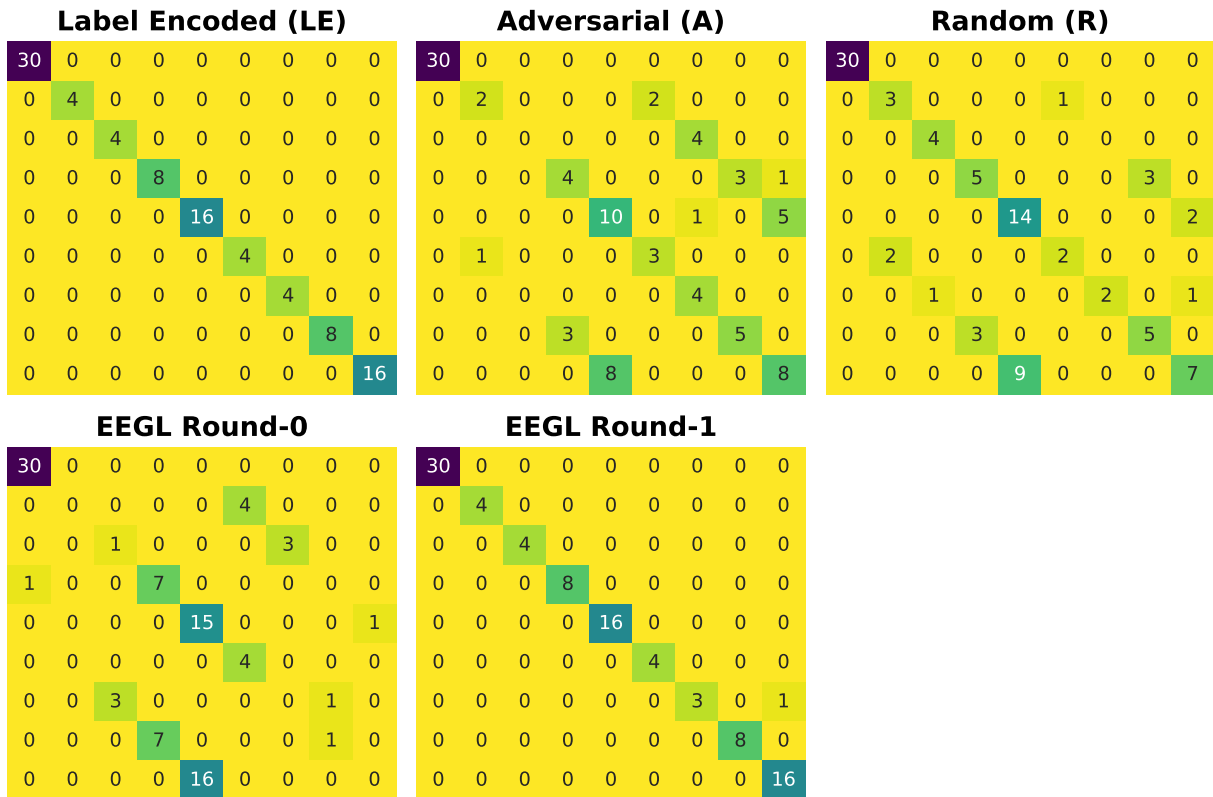


Figure 25: Confusion Matrix for fold-10

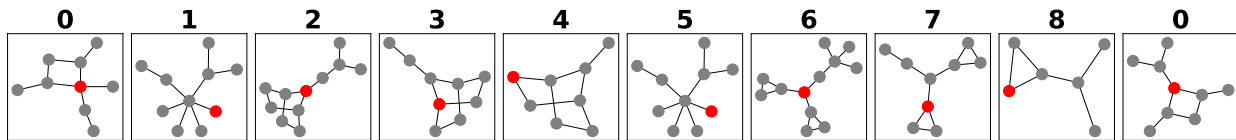


Figure 26: Top-K patterns for fold-10 from round-0 explanations. These patterns were used to annotate features for round-1